CONTENTS

NASA Technical Paper 1001

Finite-Difference Theory for Sound Propagation in a Lined Duct With Uniform Flow Using the Wave Envelope Concept

Kenneth J. Baumeister

AUGUST 1977

NASA

NASA Technical Paper 1001

Finite-Difference Theory for Sound Propagation in a Lined Duct With Uniform Flow Using the Wave Envelope Concept

Kenneth J. Baumeister

Lewis Research Center
Cleveland, Ohio

National Aeronautics
and Space Administration

Scientific and Technical
Information Office

1977

FINITE-DIFFERENCE THEORY FOR SOUND PROPAGATION IN A LINED DUCT WITH UNIFORM FLOW USING THE WAVE ENVELOPE CONCEPT

by Kenneth J. Baumeister

Lewis Research Center

SUMMARY

The finite-difference equations are derived for sound propagation in a two-dimensional, straight, soft-wall duct with a uniform flow by using the wave envelope concept. This concept involves a transformation of the wave equation into a form whose solution does not oscillate in the axial direction. This transformation reduces the required number of finite-difference grid points by one to two orders of magnitude. In this report, the governing acoustic-difference equations in complex notation are derived. Also, a new exit condition is developed that allows a duct of finite length to simulate the wave propagation in an infinitely long duct. Sample calculations are presented for a plane wave incident upon the acoustic liner. They show the numerical theory to be in good agreement with closed-form analytical theory. Also, complete pressure and velocity printouts are given to some sample problems and can be used to debug and check future computer programs.

INTRODUCTION

Finite-difference techniques are now being considered for application in complex situations involving sound propagation in ducts with axial variations in Mach number and impedance, as well as variations in duct geometry. Before these more complex problems are attempted, the finite-difference theory is applied to the simpler problems of noise propagation in ducts without flow and with steady uniform flow.

In the absence of flow, numerical theories were successfully applied to straight ducts (refs. 1 to 4), variable-area ducts (ref. 5), and ducts with variations in the wall impedance (refs. 6 and 7). Most recently, numerical techniques were applied to noise propagation in turbofan variable-area inlets with hard walls (ref. 8). Reference 3 developed the difference equations for noise propagation in an acoustically lined duct with uniform mean flow. Results were presented for a soft-wall duct in the absence of graz-

ing flow and for a hard-wall duct with grazing flow. However, reference 3 did not present any results for a soft-wall duct with mean flow because the soft-wall difference equations had not been completely programmed and debugged when reference 3 was presented.

For long ducts with relatively large attenuations, the theory and equations developed in reference 3 to simulate an infinite duct appear to be valid, based on a comparison of the finite-difference theory of reference 3 with the closed-form analytical solution of reference 9 (table XII). However, for short ducts with a length-height ratio less than 1, the numerical and analytical solutions were not in agreement. The transverse acoustic velocity calculated from the wall impedance condition was not equal to the same velocity calculated from the momentum equation. A large difference existed even though the two approaches should have yielded the same velocity at the wall. A number of possible causes were investigated, with the result that this problem finally was traced to the exit difference equation presented in reference 3. This report seeks to resolve the problem by deriving the exit condition that is valid for all duct length-height ratios.

For long ducts or high-frequency sound propagation, many grid points are necessary for a proper numerical simulation. The large number of grid points necessitates large computer storage and long execution time. To determine the optimum liner impedance, many duct calculations are usually required in a search for the impedance that gives the highest duct attenuation. This considerably extends the computer running time. A wave envelope concept was developed (ref. 6) that greatly reduced the computer running time and storage requirements.

In this report the wave envelope concept is applied to the case of uniform flow in lined ducts. The wave envelope concept was first developed in references 4 and 6 for noise propagation in ducts in the absence of flow. Kaiser and Nayfeh (ref. 10) later extended this technique to include wave propagation in variable-area ducts, again in the absence of flow.

The wave envelope concept attempts to remove most (if not all) of the axially oscillatory part of the wave pressure profile and thereby to reduce the number of grid points required for a finite-difference solution. Rather than determining the actual pressure, the wave envelope concept transforms the governing equations such that they describe the envelope of the pressure. The number of grid points can be reduced by one order of magnitude. Reduction of grid points by two orders of magnitude is possible for problems with large duct length-height ratios and high frequencies.

The derivation for the complete set of difference equations in complex notation is presented, as well as many of the details in the matrix solution. The complex form of the difference equations is simpler to program than the real form used in reference 3. These details are included so that the numerical techniques can be conveniently programmed. Sample calculations are presented, and complete pressure and velocity printouts are given to some sample problems that can be used to debug and check computer

programs. The limitations of the theory are also discussed.

GOVERNING EQUATION AND BOUNDARY CONDITION

The propagation of sound in a duct is described by a solution of the continuity and momentum equations with the appropriate impedance boundary conditions. In this section, the basic governing equations and boundary conditions for a two-dimensional rectangular duct are presented. In the next section, the difference form of these equations is developed.

Continuity and Momentum Equations

The linearized equations for mass and momentum conservation can be written for a Cartesian coordinate system in the following form:

Continuity:

$$\frac{\partial P^*}{\partial t^*} + U^* \frac{\partial P^*}{\partial x^*} + \rho_0^* c_0^{*2}\left(\frac{\partial u^*}{\partial x^*} + \frac{\partial v^*}{\partial y^*}\right) = 0 \tag{1}$$

Axial (x) momentum:

$$\frac{\partial u^*}{\partial t^*} + U^* \frac{\partial u^*}{\partial x^*} = -\frac{1}{\rho_0^*}\frac{\partial P^*}{\partial x^*} \tag{2}$$

Transverse (y) momentum:

$$\frac{\partial v^*}{\partial t^*} + U^* \frac{\partial v^*}{\partial x^*} = -\frac{1}{\rho_0^*}\frac{\partial P^*}{\partial y^*} \tag{3}$$

where an asterisk denotes dimensional quantities. The assumptions involved in the derivations of equations (1) to (3) are given in reference 11, for example. (All symbols are defined in appendix A.)

As customary for steady state, the solutions for the dependent pressures and velocities are assumed to be of the form

$$P^*(x^*, y^*, t^*) = P'(x^*, y^*)e^{i\omega^* t^*} \tag{4}$$

$$u^*(x^*, y^*, t^*) = u'(x^*, y^*)e^{i\omega^* t^*} \tag{5}$$

$$v^*(x^*, y^*, t^*) = v'(x^*, y^*)e^{i\omega^* t^*} \tag{6}$$

where a prime denotes dimensional quantities with the time-dependency removed). The final solution will be represented by the real parts of the preceding quantities. Substituting equations (4) to (6) into equations (1) to (3) and introducing the dimensionless parameters

$$P = \frac{P'}{P_A^*} \tag{7}$$

$$u = \left(\frac{\rho_0^* \omega^* H^*}{P_A^*}\right)u'; \qquad v = \left(\frac{\rho_0^* \omega^* H^*}{P_A^*}\right)v'; \qquad M = \frac{U^*}{c_0^*} \tag{8}$$

$$x = \frac{x^*}{H^*}; \qquad y = \frac{y^*}{H^*} \tag{9}$$

yield the dimensionless steady-state conservation equations

$$P - \left(\frac{iM}{2\pi\eta}\right)\frac{\partial P}{\partial x} - \frac{i}{(2\pi\eta)^2}\left(\frac{\partial u}{\partial x} + \frac{\partial v}{\partial y}\right) = 0 \tag{10}$$

$$u = i\,\frac{\partial P}{\partial x} + \frac{iM}{2\pi\eta}\,\frac{\partial u}{\partial x} \tag{11}$$

$$v = i\,\frac{\partial P}{\partial y} + \frac{iM}{2\pi\eta}\,\frac{\partial v}{\partial x} \tag{12}$$

The dimensionless frequency η is given as

$$\eta = \frac{\omega^*}{2\pi}\,\frac{H^*}{c_0^*} = \frac{f^* H^*}{c_0^*} \tag{13}$$

The dimensionless height y ranges between 0 and 1, and the dimensionless length x between 0 and the dimensionless duct length L^*/H^*.

Wave Equation

Equations (10) to (12) yield the dimensionless wave equation for uniform flow:

$$(1 - M^2)\left(\frac{\partial^2 P}{\partial x^2}\right) + \frac{\partial^2 P}{\partial y^2} + (2\pi\eta)^2 P - i4\pi\eta M \frac{\partial P}{\partial x} = 0 \tag{14}$$

Equation (14) in difference form could be solved to determine the pressure in the duct.

In the exponential notation displayed in equations (4) to (6), the dimensionless pressure and velocities in general have both real and imaginary parts. Thus,

$$P(x, y) = P^{(1)}(x, y) + iP^{(2)}(x, y) \tag{15}$$

$$u(x, y) = u^{(1)}(x, y) + iu^{(2)}(x, y) \tag{16}$$

$$v(x, y) = v^{(1)}(x, y) + iv^{(2)}(x, y) \tag{17}$$

Therefore, each term in the wave equation (eq. (14)) is complex and requires special consideration in obtaining a solution.

Wave Envelope Concept

To remove most (if not all) of the axially oscillatory part of the wave pressure profile, the pressure P is transformed into a new variable p that changes slowly in the axial direction. This new pressure p is defined as

$$P(x, y) = p(x, y)e^{(-I2\pi/\lambda^+)x} = p(x, y)e^{[-I2\pi\eta^+/(1+M)]x} \tag{18}$$

where P is the acoustic pressure and p the pressure of the wave envelope. The real parts of P and p are shown in figure 1. The effective axial wavelength parameter λ^+ is the wavelength of the oscillation in the soft-wall duct represented by figure 1. The wave envelope frequency parameter η^+ is the effective frequency of this pressure wave and is related to λ^+ as

$$\lambda^+ \equiv \frac{1 + M}{\eta^+} \tag{19}$$

This relationship was assumed because in a hard-wall duct, λ^+, Mach number M, and η^+ are exactly related as in equation (19) for plane-wave propagation.

In a soft-wall duct with sound propagating at a frequency of η, the effective frequency η^+, which would remove the oscillation according to equation (18), is not known. However, work performed in references 4 and 6 indicates that η^+ can be approximated by η. Therefore, in most problems, η^+ will be chosen equal to η. However, since this may not always be the case, η^+ is not set equal to η; rather, it is carried along in general form.

Substituting equation (18) into the wave equation (14) yields a new governing differential equation called the generalized wave envelope equation:

$$K_1 \frac{\partial^2 p}{\partial x^2} + \frac{\partial^2 p}{\partial y^2} + K_2 p + K_3 \frac{\partial p}{\partial x} = 0 \tag{20}$$

where

$$K_1 = 1 - M^2 \tag{21}$$

$$K_2 = (2\pi\eta)^2 \left[1 - \frac{(1 - M)}{(1 + M)}\left(\frac{\eta^+}{\eta}\right)^2 - \frac{2M}{1 + M}\frac{\eta^+}{\eta}\right] \tag{22}$$

$$K_3 = -i4\pi\eta\left[M + \frac{\eta^+}{\eta}(1 - M)\right] \tag{23}$$

Examples are presented to illustrate how equation (20) can remove the oscillatory nature of the pressure and thereby reduce the number of grid points necessary for a finite-difference solution.

In soft-wall ducts, λ^+ is not known precisely; therefore, the problem of picking λ^+ (or η^+) to remove the pressure oscillation must be considered. The uniform hard-wall duct, for which the correct answer is known, will now be investigated to determine the sensitivity of the final answer to the assumed value (guess) of η^+.

For plane waves propagating in hard-wall infinite ducts in the absence of flow, the wave envelope equation reduces to

$$\frac{\partial^2 p}{\partial x^2} + (2\pi)^2\left(\eta^2 - {\eta^+}^2\right)p - i4\pi\eta^+ \frac{\partial p}{\partial x} = 0 \tag{24}$$

The exact analytical solution of equation (24) for the wave envelope pressure p is

$$p = p^{(1)} + ip^{(2)} = \cos 2\pi(\eta - \eta^{+})x - i \sin 2\pi(\eta - \eta^{+})x \qquad (25)$$

The product of equation (25) with $e^{-i2\pi\eta^{+}x}$ gives the exact pressure fluctuation as defined by equation (18):

$$P = pe^{-i2\pi\eta^{+}x} = P^{(1)} + iP^{(2)} = \cos 2\pi\eta x - i \sin 2\pi\eta x \qquad (26)$$

which is independent of the choice of η^{+}, by definition.

The analytical solutions for $p^{(1)}$ from equation (25) for various assumed values of η^{+} or $|\eta - \eta^{+}|$ are shown in figure 2. For $\eta^{+} = 0$, equation (25) reduces directly to equation (26); that is, $p^{(1)}$ equals $P^{(1)}$, see the cosine-shape line in figure 2. For this assumption, about 12 grid points would be required to describe this pressure profile adequately in a difference analysis. However, if, for example, η^{+} is assumed to have a value between 0.7 and 1.3 such that $|\eta - \eta^{+}| < 0.3$, the exact analytical solution for $p^{(1)}$ would require as few as three grid points in the difference analysis. The curves for η^{+} between 1.0 and 1.3 are the mirror image of those between 0.7 and 1.0, and therefore are not shown. If η^{+} is assumed to be equal to η, the curve for $p^{(1)}$ is the straight line $\eta^{+} = 1$, or $|\eta - \eta^{+}| = 0$. This line represents the envelope of the pressure oscillation. If, for example, it is assumed that $\eta^{+} = 0.8$, the exact solution in figure 2 does not represent the true envelope of the pressure oscillation; it is still a gently varying function that requires only a few finite-difference grid points to describe its shape accurately. Thus, it is necessary only to pick a value of λ^{+} (or η^{+}) in the vicinity of the true value of λ^{+} to get a savings in the grid points required for a finite-difference analysis. In so doing, the differential Helmholtz equation is transformed to a new form (eq. (20)) that requires fewer grid points in its solution.

As another example of how to pick η^{+}, consider the problem of predicting the attenuation in a soft-wall duct, where η^{+} is an unknown. Calculations for the attenuation were made in reference 4 by assuming that $\eta^{+} = \eta$. Figure 3 (from ref. 4) shows a comparison of the analytical and wave envelope calculations for the optimum soft-wall duct attenuation for various η and L^{*}/H^{*} values.

Excellent agreement between the analytical and numerical calculations was obtained for the two-dimensional duct example in reference 4. For the $\eta = 5$ and $L^{*}/H^{*} = 6$ case in figure 3, the conventional finite-difference theory required 3600 grid points; the wave envelope difference theory required only 100 grid points. Thus, a savings of 3500 grid points over the conventional difference theory was obtained. At lower η and L^{*}/H^{*}, the savings was smaller.

In principle, any choice of η^{+} will yield the correct answer; however, a poor

choice of η^+ will require more grid points than a good choice. Thus, for any assumed value of η^+, it is necessary to check for a converged answer by increasing the number of grid points in both the x and y directions, as was done in reference 4.

Wall Boundary Condition

The boundary condition at the surface of a soft-wall duct requires that at the wall the acoustic displacement of a particle in the fluid just outside the soft wall be equal to the displacement of a particle just inside the soft wall (ref. 11). In addition, the pressure and velocity fields at the boundary can be related in terms of the specific acoustic impedance ζ, where

$$\zeta = \frac{Z^*}{\rho_0^* c_0^*} = \frac{2\pi\eta P}{v_w} \tag{27}$$

As a consequence of these two relationships, the fluid velocity at the wall is

$$v\Big|_w = \frac{2\pi\eta}{\zeta}\left(P - \frac{iM}{2\pi\eta}\frac{\partial P}{\partial x}\right)_w \tag{28}$$

and the transverse pressure gradient at the wall is

$$\frac{\partial P}{\partial y}\Bigg|_w = \frac{-i2\pi\eta P}{\zeta} - \frac{2M}{\zeta}\frac{\partial P}{\partial x}\Bigg|_w + \frac{iM^2}{\zeta 2\pi\eta}\frac{\partial^2 P}{\partial x^2}\Bigg|_w \tag{29}$$

The derivations for equations (28) and (29) are given in appendix B, equations (B12) and (B13), respectively.

Substituting the expression for the transformed pressure (eq. (18)) into equation (29) yields

$$\frac{\partial p}{\partial y}\Bigg|_w = \left(W_1 p + W_2\frac{\partial p}{\partial x} + W_3\frac{\partial^2 p}{\partial x^2}\right)\Bigg|_w \tag{30}$$

where

$$W_1 = \frac{-i2\pi\eta}{\zeta}\left[1 - \frac{2M}{1 + M}\left(\frac{\eta^+}{\eta}\right) + \frac{M^2}{(1 + M)^2}\left(\frac{\eta^+}{\eta}\right)^2\right] \tag{31}$$

$$W_2 = \frac{-2M}{\zeta}\left[1 - \frac{M}{1 + M}\left(\frac{\eta^+}{\eta}\right)\right] \tag{32}$$

$$W_3 = \frac{iM^2}{\zeta 2\pi\eta} \tag{33}$$

Exit Boundary Condition

The exit impedance must be specified at either the duct exit or some point in the far field. The exit impedance presented here will allow the numerical solution to approximate the analytical results for wave propagation in an infinitely long duct. The wave propagation in the entrance region of an infinite duct can be represented by a finite duct length L^* by choosing the exit impedance at L^* so that no reflections occur. For a plane wave propagating in a hard-wall duct with uniform mean flow, the condition for no reflections at the duct exit is an impedance of $\rho_0^* c_0^*$, or

$$\left.\begin{aligned} \zeta_e &= \frac{Z_e^*}{\rho_0^* c_0^*} = \frac{2\pi\eta P_e}{u_e} = 1 \\ x &= x_e = \frac{L^*}{H^*} \end{aligned}\right\} \tag{34}$$

In the limiting case of zero flow (refs. 2 and 4) and for uniform flow in long ducts, calculations indicate that equation (34) is a reasonable approximation for soft-wall ducts.

The axial pressure gradient at the exit can be related to the pressure at the exit by using the exit impedance condition to eliminate the acoustic velocities from the boundary condition. This is necessary since the exit condition is to be used in conjunction with the wave equation, which contains only pressure terms. Combining equation (34) with the continuity equation and the two momentum equations (see appendix C for derivation) yields the following exit condition (eq. (C15)):

$$\left.\frac{\partial P}{\partial x}\right|_e = \frac{-i2\pi\eta\left(\frac{1}{\zeta_e} - M\right)}{1 - M^2} P_e + \frac{iM\left(1 + \frac{M}{\zeta_e}\right)}{2\pi\eta(1 - M^2)} \cdot \left.\frac{\partial^2 P}{\partial y^2}\right|_e \tag{35}$$

Reference 3 used the exit equation for an infinite, one-dimensional, hard-wall duct; consequently, the second term in equation (35) was neglected. As mentioned in the INTRODUCTION, the failure of the earlier formulation to predict accurate transverse velocities in short ducts, $L^*/H^* < 1$, was traced to the neglect of the second term in equation (35).

Again, substituting the expression for the transformed pressure (eq. (18)) into equation (35) yields

$$\left.\frac{\partial p}{\partial x}\right|_e = L_1 p + L_2 \left.\frac{\partial^2 p}{\partial y^2}\right|_e \tag{36}$$

where

$$L_1 = \frac{-i2\pi\eta}{1 + M}\left(\frac{\frac{1}{\zeta_e} - M}{1 - M} - \frac{\eta^+}{\eta}\right) \tag{37}$$

$$L_2 = \frac{iM}{2\pi\eta(1 - M)}\left(\frac{1 + \frac{M}{\zeta_e}}{1 + M}\right) \tag{38}$$

In the sample calculations to follow, ζ_e will be taken as 1.

Because of the nature of the finite-difference approximations to be presented later, equation (30) cannot be used at the exit of the duct. At the exit corner of the duct, the transverse gradient at the wall is given as (eq. (D39), appendix D)

$$\left.\frac{\partial P}{\partial y}\right|_{\text{wall exit}} = \frac{-i2\pi\eta P}{\left(1 + \frac{M}{\zeta_e}\right)\zeta} - \frac{M}{\left(1 + \frac{M}{\zeta_e}\right)\zeta} \left.\frac{\partial P}{\partial x}\right|_{\text{wall exit}} \tag{39}$$

Equation (39) is a new equation; it was not previously developed. Equation (39) includes both the wall impedance ζ and the impedance at the exit ζ_e. The derivation of equation (39) and its full rationale are discussed in detail in appendix D.

Substituting the expression for the transformed pressure (eq. (18)) into equation (39) yields

$$\left.\frac{\partial p}{\partial y}\right|_{\text{wall exit}} = \left(N_1 p + N_2 \frac{\partial p}{\partial x}\right)_{\text{wall exit}} \tag{40}$$

where

$$N_1 = \frac{-i2\pi\eta}{\left(1 + \frac{M}{\zeta_e}\right)\zeta}\left[1 - \frac{M}{1 + M}\left(\frac{\eta^+}{\eta}\right)\right] \tag{41}$$

$$N_2 = \frac{-M}{\left(1 + \frac{M}{\zeta_e}\right)\zeta} \tag{42}$$

Entrance Conditions

At the entrance, a uniform pressure profile

$$P(0, y) = 1 \tag{43}$$

is used. A more general entrance condition, where $P(0, y)$ depends on y, is equally easy to treat. In terms of the envelope pressure p, equation (43) becomes

$$p(0, y) = 1 \tag{44}$$

Axial Acoustic Power

The sound power that leaves a duct and reaches the far field is related to the instantaneous axial intensity at the duct exit. On the basis of the discussion in references 12 and 13, the intensity can be expressed as

$$I_x^* = (1 + M^2)P^*u^* + \frac{MP^{*2}}{c_0^*\rho_0^*} + Mc_0^*\rho_0^*u^{*2} \qquad (45)$$

This equation is an improvement on Ryshov and Shefter's intensity equation (ref. 14), which was used in reference 3. The time-averaged intensity over a cycle is

$$I_x = \frac{2\rho_0^* c_0^*}{P_A^{*2}} I_x^* = \mathrm{Real}\left(\frac{1 + M^2}{2\pi\eta} P\bar{u}\right) + MP\bar{P} + \frac{M}{(2\pi\eta)^2} u\bar{u} \qquad (46)$$

where the bar denotes the complex conjugate.

Assuming that the axial velocity can also be expressed in wave envelope form as

$$u = u_a e^{[-i2\pi\eta^+/(1+M)]x} \qquad (47)$$

and using equations (18) and (47) give the expression for the time-averaged intensity as

$$I_x = \mathrm{Real}\left(\frac{1 + M^2}{2\pi\eta} p\bar{u}_a\right) + Mp\bar{p} + \frac{M}{(2\pi\eta)^2} u_a\bar{u}_a \qquad (48)$$

Thus, the formula for intensity in terms of p and u_a has the same functional form as equation (46).

The total dimensionless acoustic power is the integral of the intensity across the test section

$$E_x = \int_0^1 I_x(x, y)dy \qquad (49)$$

By definition, the sound attenuation (the decrease in decibels of the acoustic power from $x = 0$ to x) can be written as

$$\Delta\ \mathrm{dB} = 10 \log_{10}\left(\frac{E_x}{E_0}\right) \qquad (50)$$

Pressure Amplitude and Sound Pressure Level

The pressure amplitude $|P|$ is a useful quantity to indicate how the acoustic pres- sure varies in the duct. By definition,

$$|P| = \sqrt{P^{(1)^2} + P^{(2)^2}} \qquad (51)$$

In terms of the wave envelope pressure p,

$$|P| = \sqrt{p^{(1)^2} + p^{(2)}} \qquad (52)$$

FINITE-DIFFERENCE FORMULATION

Instead of a continuous solution for pressure, the pressure is determined at isolated grid points by means of the finite-difference approximations, as shown in figure 4. Thus, the differential equations can be changed to a system of algebraic equations in terms of the pressure at each point. This set of algebraic equations can be solved simultaneously to determine the pressure at each grid point.

Difference Equations

The governing difference equations can be developed by an integration process in which the wave envelope equation (eq. (20)) is integrated over the area of the cells shown in figure 4.

$$\iint_{\text{Cell area}} \left(K_1 \frac{\partial^2 p}{\partial x^2} + \frac{\partial^2 p}{\partial y^2} + K_2 p + K_3 \frac{\partial p}{\partial x}\right) dx\, dy = 0 \qquad (53)$$

The finite-difference approximations for the various cells shown in figure 4 are expressed in terms of the coefficients

$$a_k p_{i-1,j} + b_k p_{i,j-1} + c_k p_{i,j} + d_k p_{i,j+1} + e_k p_{i+1,j} = 0 \qquad (54)$$

The subscript k denotes the cell number. The derivation and expressions for the co-

efficients are given in appendix D. These coefficients are listed in table I.

Matrix Solution

The collection of the various difference equations at each grid point forms a set of simultaneous equations that can be expressed as

$$\{A\}[p] = [F] \tag{55}$$

where $\{A\}$ is the known coefficient matrix, $[p]$ is the unknown pressure vector, and $[F]$ is the known column vector containing the various initial conditions. The matrix is complex.

To illustrate the detailed structure of the matrix given by equation (55), consider the example shown in figure 5. For this case the detailed matrix structure becomes

$$\left[\begin{array}{cccc|cccc|cccc|cccc|cccc}
c_3 & d_3 & & & e_3 \\
b_1 & c_1 & d_1 & & & e_1 & & & & 0 & & & & 0 & & & & 0 \\
& b_1 & c_1 & d_1 & & & e_1 \\
& & b_2 & c_2 & & & & e_2 \\ \hline
a_3 & & & & c_3 & d_3 & & & e_3 \\
& a_1 & & & b_1 & c_1 & d_1 & & & e_1 & & & & 0 & & & & 0 \\
& & a_1 & & & b_1 & c_1 & d_1 & & & e_1 \\
& & & a_2 & & & b_2 & c_2 & & & & e_2 \\ \hline
& & & & a_3 & & & & c_3 & d_3 & & & e_3 \\
& 0 & & & & a_1 & & & b_1 & c_1 & d_1 & & & e_1 & & & & 0 \\
& & & & & & a_1 & & & b_1 & c_1 & d_1 & & & e_1 \\
& & & & & & & a_2 & & & b_2 & c_2 & & & & e_2 \\ \hline
& & & & & & & & a_3 & & & & c_3 & d_3 & & & e_3 \\
& 0 & & & & 0 & & & & a_1 & & & b_1 & c_1 & d_1 & & & e_1 \\
& & & & & & & & & & a_1 & & & b_1 & c_1 & d_1 & & & e_1 \\
& & & & & & & & & & & a_2 & & & b_2 & c_2 & & & & e_2 \\ \hline
& & & & & & & & & & & & a_6 & & & & c_6 & d_6 \\
& 0 & & & & 0 & & & & 0 & & & & a_4 & & & b_4 & c_4 & d_4 \\
& & & & & & & & & & & & & & a_4 & & & b_4 & c_4 & d_4 \\
& & & & & & & & & & & & & & & a_5 & & & b_5 & c_5
\end{array}\right]
\begin{bmatrix} p_{11} \\ p_{12} \\ p_{13} \\ p_{14} \\ \hline p_{21} \\ p_{22} \\ p_{23} \\ p_{24} \\ \hline p_{31} \\ p_{32} \\ p_{33} \\ p_{34} \\ \hline p_{41} \\ p_{42} \\ p_{43} \\ p_{44} \\ \hline p_{51} \\ p_{52} \\ p_{53} \\ p_{54} \end{bmatrix}
=
\begin{bmatrix} -a_3 \\ -a_1 \\ -a_1 \\ -a_2 \\ \hline 0 \\ 0 \\ 0 \\ 0 \\ \hline 0 \\ 0 \\ 0 \\ 0 \\ \hline 0 \\ 0 \\ 0 \\ 0 \\ \hline 0 \\ 0 \\ 0 \\ 0 \end{bmatrix} \tag{56}$$

where the derivation of the coefficients is given in appendix D. The dashed lines illustrate where the matrix can be partitioned into a form that is tridiagonal, which in more abbreviated notation becomes

$$
\left[\begin{array}{c:c:c:c:c}
B_1 & C_1 & 0 & 0 & 0 \\ \hdashline
A_1 & B_2 & C_2 & 0 & 0 \\ \hdashline
0 & A_3 & B_3 & C_3 & 0 \\ \hdashline
0 & 0 & A_4 & B_4 & C_4 \\ \hdashline
0 & 0 & 0 & A_5 & B_5
\end{array}\right]
\left[\begin{array}{c}
p_1 \\ \hdashline p_2 \\ \hdashline p_3 \\ \hdashline p_4 \\ \hdashline p_5
\end{array}\right]
\left[\begin{array}{c}
F_1 \\ \hdashline 0 \\ \hdashline 0 \\ \hdashline 0 \\ \hdashline 0
\end{array}\right]
\tag{57}
$$

This can be generalized for any number of points as

$$
\begin{bmatrix}
B_1 & C_1 & & & & & \\
A_2 & B_2 & C_2 & & & 0 & \\
& A_3 & B_3 & C_3 & & & \\
& & \ddots & \ddots & \ddots & & \\
& & & A_i & B_i & C_i & \\
& 0 & & & \ddots & \ddots & \ddots \\
& & & & A_{n-1} & B_{n-1} & C_{n-1} \\
& & & & A_n & B_n & C_n
\end{bmatrix}
\begin{bmatrix}
p_1 \\ p_2 \\ p_3 \\ \vdots \\ p_i \\ \vdots \\ p_{n-1} \\ p_n
\end{bmatrix}
=
\begin{bmatrix}
F_1 \\ 0 \\ 0 \\ \vdots \\ 0 \\ \vdots \\ 0 \\ 0
\end{bmatrix}
\tag{58}
$$

The difference equations are cast in this form and solved by using the computer program written by Quinn (ref. 5), which directly inverts the matrix. The solution of the matrix gives the pressure at each of the grid points. These pressures can then be used to determine the acoustic velocities and intensities throughout the duct.

ACOUSTIC PARTICLE VELOCITIES

The axial and transverse momentum equations are solved to determine the acoustic velocities in the duct. In turn, these velocities, in conjunction with the acoustic pressure, are used to determine the intensity levels in the duct and the attenuation that the duct provides.

Axial Velocity

The axial momentum (eq. (11)) can be rewritten as

$$\frac{\partial u}{\partial x} + i\beta u = -\beta \frac{\partial P}{\partial x} \tag{59}$$

where

$$\beta = \frac{2\pi\eta}{M} \tag{60}$$

In terms of the transformed pressures and axial velocities, substituting equations (18) and (47) into equation (59) yields

$$\frac{\partial u_a}{\partial x} + i\beta\left(1 - \frac{\sigma}{\beta}\right)u_a = -\beta \frac{\partial p}{\partial x} + i\beta\sigma p \tag{61}$$

where

$$\sigma = \frac{2\pi\eta^+}{1 + M} \tag{62}$$

Runge-Kutta solution. - Since the axial pressure gradient in equation (61) can be obtained directly from the numerical solution, equation (61) was treated as a simple or-

dinary differential equation. As a result, a standard fourth-order Runge-Kutta integration was used to solve equation (61). The initial condition used for the solution was found by rewriting equation (34) for $\zeta_e = 1$ as

$$u_e = 2\pi\eta P_e \tag{63}$$

$$u_a\Big|_e = 2\pi\eta P\Big|_e \tag{64}$$

The Runge-Kutta technique worked well when the wave envelope technique was not used; however, this technique became unstable in many cases when the wave envelope technique was applied. The instabilities resulted from the large steps in the independent variable x that were used in conjunction with the wave envelope approach. To correct this problem, an exact solution to equation (61) was employed.

<u>Integral solution</u>. - The problem associated with the Runge-Kutta solution could be circumvented by using an integration technique. Solving equation (61) and applying boundary condition (64) yield

$$u_a(x, y) = 2\pi\eta P(x_e, y)e^{i\varphi(x_e - x)} + \beta e^{-i\varphi x} \int_x^{x_e} e^{i\varphi s} \frac{\partial p(s, y)}{\partial s}\, ds$$

$$- i\beta\sigma e^{-i\varphi x} \int_x^{x_e} e^{i\varphi s}\, p(s, y)ds \tag{65}$$

where

$$\varphi = \beta - \sigma \tag{66}$$

Equation (65) has a disadvantage in that the pressure gradient is required for the integration process. However, equation (65) can be further simplified by integration by parts. Recognizing that

$$\int_x^{x_e} \frac{\partial}{\partial s}\left[e^{i\varphi s}\, p(s, y)\right] ds = e^{i\varphi x_e}\, p(x_e, y) - e^{i\varphi x}\, p(x, y) \tag{67}$$

and that

$$\int_x^{x_e} e^{i\varphi s} \frac{\partial p(s,y)}{\partial s} ds = e^{i\varphi x_e} p(x_e, y) - e^{i\varphi x} p(x,y) - i\varphi \int_x^{x_e} e^{i\varphi s} p(s,y)ds \quad (68)$$

and substituting equation (68) into equation (65) result in the following expression for the axial velocity:

$$u_a(x,y) = 2\pi\eta\left(1 + \frac{1}{M}\right)e^{i\varphi(x_e - x)} p(x_e, y) - \beta p(x,y) - i\beta^2 e^{-i\varphi x}\int_x^{x_e} e^{i\varphi s} p(s,y)ds \quad (69)$$

The advantage of equation (69) over equation (65) is that the integrand can be found directly from the pressure field.

The velocity at any point can be found from equation (69) by using the values of the pressure field from the solution of equation (55). Evaluating the integral in equation (69) can be a problem. The parameter φ in equation (69) can be written

$$\varphi = \frac{2\pi\eta}{M}\left[1 - \frac{M}{1+M}\left(\frac{\eta^+}{\eta}\right)\right] \quad (70)$$

Therefore, the integral term in equation (69) can be written as

$$\int_x^{x_e} e^{i\varphi s} p(s,y)ds = \int_x^{x_e} p(s,y)\exp\left[i\frac{2\pi\eta}{M}\left(1 - \frac{M}{1+M}\frac{\eta^+}{\eta}\right)s\right]ds \quad (71)$$

The exponential in equation (71) represents an oscillating function whose wavelength can be considerably shorter than the wavelength associated with the pressure field. In fact, in the limit of small Mach numbers, the wavelength associated with the exponential in equation (71) approaches zero, but the wavelength of the pressure wave is simply the inverse of η.

To illustrate this more vividly, consider the example of a soft-wall duct with a dimensionless frequency η of 1, an L^*/H^* of 3, and a Mach number of 0.5. A typical $P^{(1)}$ pressure profile in a suppressor duct is shown in figure 6(a) by the dashed lines; the solid lines denote the amplitude of the exponential $e^{i\varphi x}$. Figure 6(b) shows similar results when the wave envelope concept is used. In general, as well as in this example, the grid spacing in the finite-difference theory is chosen sufficiently small so that the pressure field can be accurately determined. The grid spacing associated with the accurate determination of the pressure field will usually be too coarse to adequately evaluate the integral in equation (71) by a conventional numerical integration formula

such as Simpson's rule. Using a larger number of grid points would be wasteful, in general and, in particular, would defeat the basic idea of the wave envelope concept, which is to reduce the number of grid points. Therefore, a combined analytical and numerical technique was used to circumvent this problem.

Polynomial-exponential integration. - The integral in equation (69) was expressed as the sum of the integrals between each grid point to give

$$\int_{x}^{x_e} p(s, y)e^{-i\varphi s}\, ds = \sum_{i}^{n} \int_{x_i}^{x_i+\Delta x} p(s, y)e^{i\varphi s}\, ds \tag{72}$$

A fourth-order polynomial fit of the pressure p was constructed from the solution of the wave equation for every value of i. In turn, equation (72) could be integrated exactly. The exact formulas are given in appendix E. This technique proved very successful.

Transverse Velocity

Once the axial velocity is known, the transverse velocity can be quickly found by using the condition of irrotationality

$$\frac{\partial u}{\partial y} = \frac{\partial v}{\partial x} \tag{73}$$

which is developed in appendix C, equation (C10).

Substituting equation (73) into equation (12) gives

$$v = i\,\frac{\partial P}{\partial y} + \frac{iM}{2\pi\eta}\,\frac{\partial u}{\partial y} \tag{74}$$

Thus, the solution of the transverse velocity can be found by a simple differentiation process once u is known. As a check, the solution of the transverse velocity can also be found by solving the continuity equation (eq. (10)) and applying the boundary condition at the wall given by equation (28). This check led to the discovery of the problem discussed in the INTRODUCTION.

In terms of the wave envelope pressures, equation (74) remains unchanged, as given by

$$v_a = i\frac{\partial p}{\partial y} + \frac{iM}{2\pi\eta}\frac{\partial u_a}{\partial y} \tag{75}$$

AXIAL INTENSITY AND POWER

In terms of the difference notation, the axial intensity given by equation (48) can be written as

$$I_{i,j} = \mathrm{Real}\left(\frac{1+M^2}{2\pi\eta} p_{i,j}\bar{u}_{a,i,j}\right) + Mp_{i,j}\bar{p}_{i,j} + \frac{M}{2\pi\eta} u_{a,i,j}\bar{u}_{a,i,j} \tag{76}$$

The total power across a particular cross section, as given by equation (49), is written in difference notation as

$$E_i = \left(\frac{1}{2} I_{i,1} + \sum_{j=2}^{m-1} I_{i,j} + \frac{1}{2} I_{i,m}\right)\Delta y \tag{77}$$

By evaluating E_i at the entrance and exit positions, for use in equation (50), the sound attenuation for the duct is determined.

SAMPLE PROBLEMS

As the first example of the difference technique, consider the problem discussed in the INTRODUCTION. Recall, for small L^*/H^*, the transverse velocities as calculated from the momentum equation and boundary condition were not equal, even though the two approaches should have yielded the same velocity at the wall. An example of this discrepancy is shown in figure 7(a). Now, however, for the new exit condition (eq. (35)), the transverse velocities calculated from the momentum equation (eq. (74)) and the boundary condition (eq. (28)) are in good agreement, as shown in figure 7(b). This agreement comes about because the pressure field has changed due to the introduction of the transverse gradient in the exit condition (eq. (35)). The attenuation calculated by using the exit condition of reference 3 is 6.1; the attenuation calculated by using equation (35) as the exit condition is 3.4, which is a significant difference.

In another example of the difference technique, the noise attenuation at the optimum point (point of maximum attenuation in the impedance plane) is calculated for a two-dimensional duct with an L^*/H^* of 3.43, a Mach number of 0.3, and the ranges of the parameter η and ζ listed in table II. In figure 8, the numerically calculated attenua-

tions are compared with corresponding analytical results (ref. 9) that are applicable to infinite ducts. The numerical results (lines) and the analytical results (circular symbols) for the maximum attenuation are shown in figure 8 to be in very good agreement.

For symmetrical ducts (impedance identical at both walls), the pressure profiles are symmetrical about the centerline of the duct. In this case, $\partial P/\partial y$ can be set equal to zero at the centerline of the duct. Consequently, the number of grid points in the y-direction could be cut in half.

The deviation between the closed form and the numerical analysis shown in figure 8 at the lowest dimensionless frequency is assumed to occur because the $\rho_0^* c_0^*$ exit impedance used in the numerical analysis begins to deviate from the exit impedance in the analytical results (ref. 15, p. 246). By extending the soft-wall duct (ref. 2, appendix E), it is possible to reduce the reflected contribution and thereby more closely simulate an infinite duct, which is the basis for the analytical calculations. The dashed line in figure 8 results from increasing the duct L^*/H^* to 6.86 and evaluating the attenuation at an x of 3.43.

PROGRAMMING AIDS

Appendix F contains the solutions of four additional sample problems. Complete pressure and velocity printouts are given and can be used to debug and check the computer programs. The pressure profiles for the two standard solutions that do not use the wave envelope concept ($\eta^+ = 0$) were checked by two independent computer programs (refs. 2 and 5) that used two different techniques for solving the matrix equations. Therefore, if the same difference equations are programmed, agreement of the pressure field to three-place accuracy should be expected.

The outputs of the velocity fields are also presented in appendix F. For the uniform-velocity cases, these flow fields have not been double checked by independent programming because these solutions have been developed from the new techniques presented in this report.

LIMITATIONS OF THEORY

At low frequencies ($\eta \lesssim 0.5$), the exit impedance $\rho_0^* c_0^*$ used in this analysis does not necessarily lead to a condition of no reflection at the duct exit. Therefore, if the reflections are large, the numerical solutions will not necessarily be equal to the analytical infinite-duct results. For example, the attenuation calculated by the analytical infinite-duct theory for figure 7 was 2.0 decibels, which is 1.4 decibels lower than the numerical results. Doubling and tripling the duct length produced large oscillations in

the pressure amplitude $|P|$ in the axial direction. This oscillation was interpreted to mean that large reflections were occurring at the exit of the duct. These calculations were performed without using the wave envelope theory. At low frequencies the wave envelope theory is not required since the wavelength of the pressure is very long.

In general, a pressure wave is composed of a forward-going and a reflected wave. The present wave envelope theory is useful only in those cases where the reflected wave is small compared with the forward-going wave, since the reflective component has been neglected in equation (18). The wave envelope technique may also be limited to the case with a single dominant mode or to the special multimodal case where the modes have similar effective axial wavelengths. In all cases, in solving a particular problem by using finite-difference theory, the grid spacing should be doubled in order to check for convergence.

Finally, assuming ρ_e equals 1 in equation (34) applies strictly to a single plane wave. Therefore, some reflection will occur at the duct exit for pressure waves other than plane. However, for $\eta > 1$, this reflection is generally small.

CONCLUDING REMARKS

A finite-difference wave envelope theory for sound propagation in a two-dimensional soft-wall duct with uniform mean flow has been presented. Previous difference theory did not give valid attenuations or acoustic velocities for ducts with L^*/H^* of the order of 0.5. The difference theory with plane-wave input developed herein is shown to be in good agreement with closed-form analysis for the complete range of duct parameters.

Also given are the latest numerical procedures in applying finite-difference techniques to ducts. The derivations for the various procedures are presented in appendixes.

Lewis Research Center,

National Aeronautics and Space Administration,

Cleveland, Ohio, May 6, 1977,

505-03.

APPENDIX A

SYMBOLS

A	coefficient matrix
A_i	submatrix
a_k	matrix element
B_i	submatrix
b_k	matrix element
C	constant
C_i	submatrix
c_0^*	speed of sound, m/sec
c_k	matrix element
d_k	matrix element
ΔdB	sound attenuation, dB
E_i	total acoustic power (eq. (77))
E_x	acoustic power (eq. (49))
E_0	E_x evaluated at $x = 0$
e_k	matrix element
$\underline{F}$	initial-condition column vector
F_1	initial-condition submatrix column vector
f^*	frequency, Hz
H^*	channel height, m
I_x	acoustic-intensity axial direction
i	$\sqrt{-1}$
K_1, K_2, K_3	coefficients of generalized wave envelope equation (eq. (20))
L^*	length of duct, m
L_1, L_2	exit-condition coefficients (eq. (36))
M	Mach number, U^*/c_0^*
m	total number of grid rows
N	index: 0, 1, or 2

N_1, N_2	wall exit coefficients (eq. (40))
n	total number of grid columns
P	dimensionless pressure fluctuations $P(x, y) = P'/P_A^*$
P_i	submatrix-column pressure vector
P^*	pressure fluctuation, $P^*(x^*, y^*, t)$, N/m^2
P_A^*	amplitude of pressure fluctuation, N/m^2
P'	$P'(x^*, y^*)$, N/m^2
$\underline{P}$	pressure-column vector (eq. (55))
p	wave envelope pressure
p_{ij}	element of pressure at i, j grid point
Q_i	polynomial coefficients
s	dummy variable of integration
t^*	time, sec
U^*	mean flow velocity in x-direction, m/sec
u	dimensionless acoustic particle velocity in x-direction
u_a	dimensionless axial velocity (eq. (47))
v	dimensionless acoustic particle velocity in y-direction
v_a	dimensionless transverse velocity (eq. (75))
W_1, W_2, W_3	boundary-condition coefficients (eq. (30))
x	dimensionless axial coordinate, x^*/H^*
x_0	starting grid position for polynomial fit
Δx	axial grid spacing
y	dimensionless transverse coordinate, y^*/H^*
Δy	transverse grid spacing
Z^*	acoustic impedance, kg/m^2-sec
z	dummy variable of integration
α_i	coefficients of polynomial fit
β	$2\pi\eta/M$ (eq. (60))
ϵ	$1/i\varphi\ \Delta x$ (eq. (E16))
ζ	specific acoustic impedance

η dimensionless frequency

η^+ wave envelope frequency

λ^+ effective axial wavelength

ξ particle displacement

ρ_0^* density of uniform medium, kg/m^3

σ $2\pi\eta^+/(1 + M)$ (eq. (62))

Φ potential function

φ $\beta - \sigma$ (eq. (66))

ω^* circular frequency

Subscripts:

e exit condition

i axial index (fig. 4)

j transverse index (fig. 4)

k cell index

opt optimum

w wall

x axial position

y transverse position

Superscripts:

* dimensional quantity

' dimensional quantity with time function removed

$(\bar{\ })$ complex conjugate

(1) real part

(2) imaginary part

APPENDIX B

DISPLACEMENT CONDITIONS

This appendix develops the relationships between the transverse velocity just inside an acoustic absorber and the transverse velocity just outside the absorber in the fluid medium. The development follows that of reference 11. By definition, the acoustic velocity of the medium in a duct can be related to the displacement of the particle by

$$v^* = \frac{D\xi^*}{Dt} = \frac{\partial \xi^*}{\partial t^*} + U^* \frac{\partial \xi^*}{\partial x^*} \tag{B1}$$

where an asterisk denotes a dimensional quantity. Assuming a harmonic displacement and velocity of the form

$$v^* \sim \xi^* \sim e^{i\omega^* t^*} \tag{B2}$$

gives

$$v' = i\omega^* \xi' + U^* \frac{\partial \xi}{\partial x^*} \tag{B3}$$

where a prime denotes a dimensional quantity with the time function removed.

With the absence of convection inside the absorbing wall, the transverse velocity can be expressed as

$$v_w^* = \frac{\partial \xi_w^*}{\partial t^*} \tag{B4}$$

Again, for harmonic displacements as in equation (B2), the transverse velocity inside the wall becomes

$$v_w' = i\omega^* \xi_w' \tag{B5}$$

or

$$\xi_w' = \frac{v_w'}{i\omega^*} \tag{B6}$$

The continuity of particle displacement requires that at the interface between the absorber and the fluid

$$\xi'_w = \xi'|_w \tag{B7}$$

Combining equations (B3), (B6), and (B7) yields

$$v'|_w = v'_w + \frac{U^*}{i\omega^*}\frac{\partial v'_w}{\partial x^*} \tag{B8}$$

The impedance condition at a wall can be written as

$$\zeta = \frac{P^*}{\rho_0^* c_0^* v_w^*} \tag{B9}$$

or for harmonic displacements (eq. (B2)) the wall velocity becomes

$$v'_w = \frac{P'}{\rho_0^* c_0^* \zeta} \tag{B10}$$

Substituting equation (B10) into equation (B8) yields, for the transverse velocity at the wall in the medium,

$$v'|_w = \frac{1}{\rho_0^* c_0^* \zeta}\left(P' + \frac{U^*}{i\omega^*}\frac{\partial P'}{\partial x^*}\right) \tag{B11}$$

In dimensionless form,

$$v|_w = \frac{2\pi\eta}{\zeta}\left(P - \frac{iM}{2\pi\eta}\frac{\partial P}{\partial x}\right) \tag{B12}$$

Substituting equation (B12) into equation (12) in the main body of the report yields the displacement boundary condition at the wall,

$$\left.\frac{\partial P}{\partial y}\right|_w = \frac{-i2\pi\eta P}{\zeta} - \frac{2M}{\zeta}\left.\frac{\partial P}{\partial x}\right|_w + \frac{iM^2}{\zeta 2\pi\eta}\left.\frac{\partial^2 P}{\partial x^2}\right|_w \tag{B13}$$

APPENDIX C

EXIT CONDITION

The derivation of the exit boundary condition for a soft wall is now presented. The goal of the derivation will be to relate the axial pressure gradient at the exit to the impedance and pressure at the exit. This requires some manipulation of the continuity and momentum equations in order to eliminate the acoustic velocities from the boundary condition. This is necessary since the exit condition is to be used in conjunction with the wave equation, which contains only pressure terms.

At the exit, the impedance relationship can be written

$$\zeta_e = \frac{Z_e}{\rho_0 c_0} = \frac{2\pi\eta P}{u} \tag{C1}$$

or

$$u = \frac{2\pi\eta P}{\zeta_e} \tag{C2}$$

At the exit, the momentum equation (eq. (11)) must also hold; therefore substituting equation (11) into equation (C2) yields

$$i\frac{\partial P}{\partial x} + i\frac{M}{2\pi\eta}\frac{\partial u}{\partial x} = \frac{2\pi\eta P}{\zeta_e} \qquad \text{at the exit plane} \tag{C3}$$

The axial gradient of u in equation (C3) can be expressed in terms of the transverse velocity v by using the continuity equation. Equation (10) can be rewritten as

$$\frac{\partial u}{\partial x} = -i(2\pi\eta)^2 P - 2\pi\eta M\frac{\partial P}{\partial x} - \frac{\partial v}{\partial y} \tag{C4}$$

Substituting equation (C4) into equation (C3) yields

$$\frac{\partial P}{\partial x} = \frac{-i(2\pi\eta)\left(\frac{1}{\zeta_e} - M\right)}{1 - M^2} P + \frac{M}{2\pi\eta(1 - M^2)}\frac{\partial v}{\partial y} \tag{C5}$$

The transverse gradient term can also be expressed in terms of pressure. An expression for the transverse velocity gradient is obtained by differentiating equation (12) with respect to y.

$$\frac{\partial v}{\partial y} = i\frac{\partial^2 P}{\partial y^2} + i\frac{M}{2\pi\eta}\frac{\partial}{\partial y}\left(\frac{\partial v}{\partial x}\right) \tag{C6}$$

Substituting equation (C6) into equation (C5) yields

$$\frac{\partial P}{\partial x} = \frac{-i(2\pi\eta)\left(\frac{1}{\zeta_e} - M\right)}{1 - M^2} P + \frac{iM}{2\pi\eta(1 - M^2)}\frac{\partial^2 P}{\partial y^2} + \frac{iM^2}{(2\pi\eta)^2(1 - M^2)}\frac{\partial}{\partial y}\left(\frac{\partial v}{\partial x}\right) \quad \text{at the exit plane} \tag{C7}$$

The axial gradient in v in equation (C7) can be replaced by the transverse gradient in u. Differentiating the axial momentum equation (eq. (11)) with respect to y and the transverse momentum equation (eq. (12)) with respect to x and subtracting these equations yield

$$\frac{\partial}{\partial x}\left(\frac{\partial u}{\partial y} - \frac{\partial v}{\partial x}\right) + i\frac{2\pi\eta}{M}\left(\frac{\partial u}{\partial y} - \frac{\partial v}{\partial x}\right) = 0 \tag{C8}$$

which has a solution

$$\frac{\partial u}{\partial y} - \frac{\partial v}{\partial x} = Ce^{(-i2\pi\eta/M)x} \tag{C9}$$

Since the desired solution should also be valid at a Mach number of zero, the constant of integration is taken as zero; thus,

$$\frac{du}{dy} = \frac{dv}{dx} \tag{C10}$$

This is the condition of irrotationality that is anticipated from irrotational potential flow theory. If the potential functions $u = \partial\Phi/\partial x$ and $v = \partial\Phi/\partial y$ had been assumed, equation (C10) could have been assumed immediately without any manipulations. Substituting equation (C10) into equation (C7) yields

$$\frac{\partial P}{\partial x} = \frac{-i(2\pi\eta)\left(\frac{1}{\zeta_e} - M\right)}{1 - M^2} P + \frac{iM}{2\pi\eta(1 - M^2)} \frac{\partial^2 P}{\partial y^2} + \frac{iM^2}{(2\pi\eta)^2(1 - M^2)} \frac{\partial^2 u}{\partial y^2} \tag{C11}$$

The transverse gradient of u can be found from the exit impedance relationship. Differentiating equation (C2) with respect to y yields

$$\frac{\partial u}{\partial y} = \frac{2\pi\eta}{\zeta_e} \frac{\partial P}{\partial y} - \frac{2\pi\eta P}{\zeta_e^2} \frac{\partial \zeta_e}{\partial y} \tag{C12}$$

In this report, ζ_e is assumed to be constant and independent of y; therefore,

$$\frac{\partial u}{\partial y} = \frac{2\pi\eta}{\zeta_e} \frac{\partial P}{\partial y} \tag{C13}$$

Differentiating one more time gives

$$\frac{\partial^2 u}{\partial y^2} = \frac{2\pi\eta}{\zeta_e} \frac{\partial^2 P}{\partial y^2} \tag{C14}$$

Substituting equation (C14) into equation (C11) yields

$$\left.\frac{\partial P}{\partial x}\right|_e = \frac{-i(2\pi\eta)\left(\frac{1}{\zeta_e} - M\right)}{1 - M^2} P + \left.\frac{iM\left(1 + \frac{M}{\zeta_e}\right)}{2\pi\eta(1 - M^2)} \frac{\partial^2 P}{\partial y^2}\right|_e \tag{C15}$$

For the case under consideration in this report, $\zeta_e = 1$. Therefore, equation (C15) reduces to

$$\left.\frac{\partial P}{\partial x}\right|_e = \frac{-i(2\pi\eta)}{1 + M} P + \left.\frac{iM}{2\pi\eta(1 - M)} \frac{\partial^2 P}{\partial y^2}\right|_e \tag{C16}$$

APPENDIX D

FINITE-DIFFERENCE EQUATIONS AND COEFFICIENTS

The finite-difference equations for the various cells shown in figure 4 can be obtained by integrating the wave equation over the cell area.

$$\int_{-}^{+}\int_{-}^{+}\left(K_1 \frac{\partial^2 p}{\partial x^2} + \frac{\partial^2 p}{\partial y^2} + K_2 p + K_3 \frac{\partial p}{\partial x}\right) dx\, dy = 0 \tag{D1}$$

where the plus sign (+) in the upper limit of integration means to evaluate the parameters along either the upper or right-hand boundary of the integration cell, shown in figure 4 by the dashed lines, while the negative sign (-) applies to either the lower or left-hand boundary of the integration cell, depending on whether x or y is considered.

For convenience, equation (D1) is broken into four separate integrals

$$K_1 \int_{-}^{+}\int_{-}^{+} \frac{\partial^2 p}{\partial x^2}\, dx\, dy + \int_{-}^{+}\int_{-}^{+} \frac{\partial^2 p}{\partial y^2}\, dx\, dy + K_2 \int_{-}^{+}\int_{-}^{+} p\, dx\, dy$$

$$+ K_3 \int_{-}^{+}\int_{-}^{+} \frac{\partial p}{\partial x}\, dx\, dy = 0 \tag{D2}$$

Each of these integrals can be integrated

$$K_1 \int_{-}^{+} \frac{\partial p}{\partial x}\bigg|_{-}^{+} dy + \int_{-}^{+} \frac{\partial p}{\partial y}\bigg|_{-}^{+} dx + K_2 p_{i,j} \int_{-}^{+}\int_{-}^{+} dx\, dy$$

$$+ K_3 p\bigg|_{-}^{+}{}_{\text{x-axis}} \int_{-}^{+} dy = 0 \tag{D3}$$

The various pressures and their derivatives in equation (D3) are evaluated at the edges of the cells, designated by the + and - signs. These terms will be different for each

cell because the boundary conditions, as well as the size of the cell, vary.

Central Cell 1 (k = 1)

In this region,

$$\left.\frac{\partial p}{\partial x}\right|_{-}^{+} = \left.\frac{\partial p}{\partial x}\right|^{+} - \left.\frac{\partial p}{\partial x}\right|_{-} = \left(\frac{p_{i+1,j} - p_{i,j}}{\Delta x}\right) - \left(\frac{p_{i,j} - p_{i-1,j}}{\Delta x}\right) \tag{D4}$$

$$\left.\frac{\partial p}{\partial y}\right|_{-}^{+} = \left.\frac{\partial p}{\partial y}\right|^{+} - \left.\frac{\partial p}{\partial y}\right|_{-} = \left(\frac{p_{i,j+1} - p_{i,j}}{\Delta y}\right) - \left(\frac{p_{i,j} - p_{i,j-1}}{\Delta y}\right) \tag{D5}$$

$$p\Big|_{-}^{+} = p\Big|^{+} - p\Big|_{-} = \left(\frac{p_{i+1,j} + p_{i,j}}{2}\right) - \left(\frac{p_{i-1,j} + p_{i,j}}{2}\right) \tag{D6}$$

$$\int_{-}^{+} dx = \Delta x \tag{D7}$$

$$\int_{-}^{+} dy = \Delta y \tag{D8}$$

Substituting equations (D4) to (D6) into equation (D3), performing the required integrations, multiplying each term by $-(\Delta y/\Delta x)$, and grouping the terms into the form given by equation (54) yield the following coefficients for the difference equations:

$$a_1 = -K_1\left(\frac{\Delta y}{\Delta x}\right)^2 + K_3 \frac{(\Delta y)^2}{2\ \Delta x} \tag{D9}$$

$$b_1 = -1 \tag{D10}$$

$$c_1 = 2\left[1 + K_1\left(\frac{\Delta y}{\Delta x}\right)^2 - \frac{K_2(\Delta y)^2}{2}\right] \tag{D11}$$

$$d_1 = -1 \tag{D12}$$

$$e_1 = -K_1\left(\frac{\Delta y}{\Delta x}\right)^2 - K_3\frac{(\Delta y)^2}{2\,\Delta x} \tag{D13}$$

Upper-Wall Cell 2 (k = 2)

In this region, $\partial p/\partial x\big|_-^+$, $p\big|_-^+$, and $\int_-^+ dx$ remain the same as in cell 1. In this region, $\partial p/\partial y\big|_-^+$ takes on the value of the boundary condition given by equation (29); therefore,

$$\left.\frac{\partial p}{\partial y}\right|_-^+ = W_1 p_{i,j} + W_2\left.\frac{\partial p}{\partial x}\right|_w + W_3\left.\frac{\partial^2 p}{\partial x^2}\right|_w - \left(\frac{p_{i,j} - p_{i,j-1}}{\Delta y}\right) \tag{D14}$$

When equation (D14) is substituted into equation (D3), integrating $\partial p/\partial x\big|_w$ and $\partial^2 p/\partial x^2\big|_w$ yields

$$\int_-^+ \left.\frac{\partial p}{\partial x}\right|_w dx = p_w\Big|_-^+ = \left(\frac{p_{i+1,j} - p_{i,j}}{2}\right) - \left(\frac{p_{i-1,j} + p_{i,j}}{2}\right) \tag{D15}$$

$$\int_-^+ \left.\frac{\partial^2 p}{\partial x^2}\right|_w dx = \left.\left.\frac{\partial p}{\partial x}\right|_w\right|_-^+ = \left(\frac{p_{i+1,j} - p_{i,j}}{\Delta x}\right) - \left(\frac{p_{i,j} - p_{i-1,j}}{\Delta x}\right) \tag{D16}$$

Also,

$$\int_-^+ dy = \frac{\Delta y}{2} \tag{D17}$$

Substituting equation (D4), $\partial p/\partial y\big|_-$ from equation (D5), equation (D7), and equations (D14) to (D17) into equation (D3), performing the required integrations, and multiplying each term by $-2(\Delta y/\Delta x)$ yield the following coefficients:

$$a_2 = a_1 + W_2\frac{\Delta y}{\Delta x} - 2W_3\frac{\Delta y}{\Delta x^2} \tag{D18}$$

$$b_2 = -2 \tag{D19}$$

$$c_2 = c_1 - 2W_1 \Delta y + 4W_3 \frac{\Delta y}{\Delta x^2} \tag{D20}$$

$$d_2 = 0 \tag{D21}$$

$$e_2 = e_1 - W_2 \frac{\Delta y}{\Delta x} - 2W_3 \frac{\Delta y}{\Delta x^2} \tag{D22}$$

In equation (54), j takes on the value of m.

Lower-Wall Cell 3 (k = 3)

A similar derivation applies to the lower wall. In performing the derivation, remember that the impedance is a vector quantity and must be taken as negative at the lower wall if the outward normal of the velocity is not used at the lower wall. The following coefficients result:

$$a_3 = a_2 \tag{D23}$$

$$b_3 = 0 \tag{D24}$$

$$c_3 = c_2 \tag{D25}$$

$$d_3 = -2 \tag{D26}$$

$$e_3 = e_2 \tag{D27}$$

In equation (54), j takes on the value of 1.

Central Exit Cell Number 4 (k = 4)

In this region, $\partial p/\partial y\big|_-^+$ and $\int_-^+ dy$ remain the same as in cell 1. In this region, $\partial p/\partial x\big|^+$ takes on the value of the exit condition given by equation (36); therefore,

$$\left.\frac{\partial p}{\partial x}\right|_-^+ = L_1 p_{i,j} + L_2 \left.\frac{\partial^2 p}{\partial y^2}\right|_e - \left(\frac{p_{i,j} - p_{i-1,j}}{\Delta x}\right) \tag{D28}$$

When equation (D28) is substituted into equation (D3), integrating the $\partial^2 p/\partial y^2$ term yields

$$\int_{-}^{+} \left.\frac{\partial^2 p}{\partial y^2}\right|_e dy = \left(\frac{p_{i,j+1} - p_{i,j}}{\Delta y}\right) - \left(\frac{p_{i,j} - p_{i,j-1}}{\Delta y}\right) \tag{D29}$$

Also,

$$p\Big|_{-}^{+} = p_{i,j} - \left(\frac{p_{i,j} + p_{i-1,j}}{2}\right) \tag{D30}$$

$$\int_{-}^{+} dx = \frac{\Delta x}{2} \tag{D31}$$

Substituting equations (D5), (D8), and (D28) to (D31) into equation (D3), performing the required integrations, and multiplying each term by $-2(\Delta y/\Delta x)$ yield the following coefficients:

$$a_4 = 2a_1 \tag{D32}$$

$$b_4 = -1 - \frac{2K_1L_2}{\Delta x} \tag{D33}$$

$$c_4 = c_1 - \frac{K_3\,\Delta y^2}{\Delta x} + \frac{4K_1L_2}{\Delta x} - \frac{2K_1L_1\,\Delta y^2}{\Delta x} \tag{D34}$$

$$d_4 = -1 - \frac{2K_1L_2}{\Delta x} \tag{D35}$$

$$e_4 = 0 \tag{D36}$$

In the problem, ζ_e is 1; however, ζ_e is left in these equations in the event that a different value of ζ_e might be used at some future date. Also, in equation (54), i takes on the value of n.

Upper-Corner Exit Cell 5 (k = 5)

The corner condition combines both the exit and wall impedances in a single cell. In this region, $\partial p/\partial x|_{-}^{+}$ is again defined by equation (D28). Performing the first integration in equation (D3) yields

$$K_1 \int_{-}^{+} \frac{\partial p}{\partial x}\bigg|_{-}^{+} dy = -\frac{K_1(p_{i-1,j} - p_{i,j})\Delta y}{2\,\Delta x} + \frac{K_1 L_1 p_{i,j}\,\Delta y}{2} + K_1 L_2 \frac{\partial p}{\partial y}\bigg|_{-}^{+} \tag{D37}$$

The term $\partial p/\partial y|^{+}$ is defined by equation (30) in the body of the report. Unfortunately, the second derivative term $\partial^2 p/\partial x^2|_w$ in equation (30) can not be evaluated in this cell because only two grid points are available in the x-direction. Three grid points are required to evaluate a second-order derivative.

This problem can be circumvented by redefining the wall condition in terms of the exit impedance. At the exit, for the irrotationality condition (eq. (73)) and the impedance condition (eq. (C13)), we can write

$$\frac{\partial v}{\partial x} = \frac{\partial u}{\partial y} = \frac{2\pi\eta}{\zeta_e}\frac{\partial P}{\partial y} \tag{D38}$$

Substituting equations (D38) and (28) into equation (12) and solving for $\partial P/\partial y$ yields

$$\frac{\partial P}{\partial y}\bigg|_{\text{wall exit}} = -\frac{i2\pi\eta P}{\left(1 + \frac{M}{\zeta_e}\right)\zeta} - \frac{M}{\left(1 + \frac{M}{\zeta_e}\right)\zeta}\frac{\partial p}{\partial x}\bigg|_{\text{wall exit}} \tag{D39}$$

In terms of the transformed pressure, defined by equation (18) in the body of this report, equation (D39) becomes

$$\frac{\partial p}{\partial y}\bigg|_{\text{wall exit}} = N_1 p + N_2 \frac{\partial p}{\partial x}\bigg|_{\text{wall exit}} \tag{D40}$$

where

$$N_1 = \frac{-i2\pi\eta}{\left(1 + \frac{M}{\zeta_e}\right)\zeta}\left[1 - \frac{M}{1 + M}\left(\frac{\eta^+}{\eta}\right)\right] \tag{D41}$$

$$N_2 = \frac{-M}{\left(1 + \frac{M}{\zeta_e}\right)\zeta} \tag{D42}$$

Assuming

$$\left.\frac{\partial p}{\partial x}\right|_{\text{wall exit}} = \frac{p_{i,j} - p_{i-1,j}}{\Delta x} \tag{D43}$$

then

$$\left.\frac{\partial p}{\partial y}\right|_{-}^{+} = N_1 p_{i,j} + N_2\left(\frac{p_{i,j} - p_{i-1,j}}{\Delta x}\right) - \left(\frac{p_{i,j} - p_{i,j-1}}{\Delta y}\right) \tag{D44}$$

In addition, $p\Big|_{-}^{+}$ is the same as in cell 4 (eq. (D30)) and

$$\int_{-}^{+} dx = \frac{\Delta x}{2} \tag{D45}$$

$$\int_{-}^{+} dy = \frac{\Delta y}{2} \tag{D46}$$

Substituting equations (D30) and (D37) into equation (D3), performing the required integrations, multiplying each term by $-4(\Delta y/\Delta x)$, and grouping the terms into the form given by equation (30) yield the following coefficients:

$$a_5 = a_4 + 4K_1L_2N_2\frac{\Delta y}{\Delta x^2} + 2N_2\frac{\Delta y}{\Delta x} \tag{D47}$$

$$b_5 = 2b_4 \tag{D48}$$

$$c_5 = c_4 - 2N_1\,\Delta y - 2N_2\frac{\Delta y}{\Delta x} - 4K_1L_2N_1\frac{\Delta y}{\Delta x} - 4K_1L_2N_2\frac{\Delta y}{\Delta x^2} \tag{D49}$$

$$d_5 = 0 \tag{D50}$$

$$e_5 = 0 \tag{D51}$$

In equation (30), j takes on the value of m and i takes on the value of n.

Lower-Corner Exit Cell 6 ($k = 6$)

A similar derivation applied to the lower wall (see discussion of cell 3) yields

$$a_6 = a_5 \tag{D52}$$

$$b_6 = 0 \tag{D53}$$

$$c_6 = c_5 \tag{D54}$$

$$d_6 = d_5 \tag{D55}$$

$$e_6 = 0 \tag{D56}$$

In equation (30), j takes on the value of 1 and i takes on the value of n.

APPENDIX E

POLYNOMIAL-EXPONENTIAL INTEGRATION

The integral in equation (69) is expressed as the sum of the integrals between each grid point:

$$\int_{x}^{x_e} p(s, y)e^{i\varphi s}\, ds = \sum_{i}^{n} \int_{x_i}^{x_i+\Delta x} p(s, y)e^{i\varphi s}\, ds \tag{E1}$$

A third-order polynomial fit of the pressure p is constructed from the solution of the wave equation

$$p(s, y) = \alpha_0 + \alpha_1(s - x_0) + \alpha_2(s - x_0)^2 + \alpha_3(s - x_0)^3 \tag{E2}$$

where

Starting point:

$$x_0 = 0 \qquad \text{if } x_i = 0 \tag{E3}$$

Central points:

$$x_0 = x_i - \Delta x \qquad \text{if } 0 < x_i < x_e - \Delta x \tag{E4}$$

End point:

$$x_0 = x_i - 2\,\Delta x \qquad \text{if } x_i = x_e - \Delta x \tag{E5}$$

Substituting equation (E2) into equation (E1) gives

$$\int_{x}^{x_e} p(s, y)e^{i\varphi s}\, ds = \sum_{i}^{n} \int_{x_i}^{x_i+\Delta x} \left[\alpha_0 + \alpha_1(s - x_0) + \alpha_2(s - x_0)^2 + \alpha_3(s - x_0)^3\right]e^{i\varphi s}\, ds \tag{E6}$$

The integral of the polynomial in equation (E6) will be integrated exactly by using formulas given in standard integration tables (ref. 16). However, to simplify the integration, let

$$z = s - x_0 \tag{E7}$$

Therefore, equation (E6) becomes

$$\int_{x}^{x_e} p(s, y)e^{i\varphi s}\, ds = \sum_{i}^{n} e^{i\varphi x_0} \int_{x_i}^{x_i + \Delta x - x_0} \left(\alpha_0 + \alpha_1 z + \alpha_2 z^2 + \alpha_3 z^3\right) d^{i\varphi z}\, dz \tag{E8}$$

Furthermore, to ease the numerical integration, let

$$x_i - x_0 = N\, \Delta x \tag{E9}$$

$$x_i + \Delta x - x_0 = (N + 1)\Delta x \tag{E10}$$

where

Starting point:

$$N = 0 \qquad \text{if } \; x_i = 0 \tag{E11}$$

Central points:

$$N = 1 \qquad \text{if } \; 0 < x_i < x_e - \Delta x \tag{E12}$$

End point:

$$N = 2 \qquad \text{if } \; x_i = x_e - \Delta x \tag{E13}$$

Therefore, equation (E8) becomes

$$\int_{x}^{x_e} p(s, y)e^{i\varphi s}\, ds = \sum_{i}^{n} e^{i\varphi x_0} \int_{N\,\Delta x}^{(N+1)\Delta x} \left(\alpha_0 + \alpha_1 z + \alpha_2 z^2 + \alpha_3 z^3\right) e^{i\varphi z}\, dz \tag{E14}$$

By using equations (565. 1, 567. 1, 567. 2, and 567. 3) from reference 16, the integral for equation (E14) can be expressed as

$$\int_{x}^{x_e} p(s, y)e^{i\varphi s}\, ds = \sum_{i}^{n} \epsilon\, \Delta x e^{i\varphi x_i}\Big(\alpha_0(e^{i\varphi\, \Delta x} - 1) + \alpha_1\, \Delta x\left[e^{i\varphi\, \Delta x}(N + 1 - \epsilon) - (N - \epsilon)\right]$$

$$+ \alpha_2\, \Delta x^2\left\{e^{i\varphi\, \Delta x}\left[(N + 1)^2 - 2\epsilon(N + 1) + 2\epsilon^2\right] - (N^2 - 2\epsilon N + 2\epsilon^2)\right\}$$

$$+ \alpha_3\, \Delta x^3\Big\{e^{i\varphi\, \Delta x}\left[(N + 1)^3 - 3\epsilon(N + 1)^2 + 6\epsilon^2(N + 1) - 6\epsilon^3\right]$$

$$- (N^3 - 3\epsilon N^2 + 6\epsilon^2 N - 6\epsilon^3)\Big\}\Big) \qquad \text{(E15)}$$

where

$$\epsilon = \frac{1}{i\varphi\, \Delta x} \qquad \text{(E16)}$$

The expressions for the coefficients α_0, α_1, α_2, and α_3 can be evaluated directly from the formulas

$$\alpha_0 = Q_0 \qquad \text{(E17)}$$

$$\alpha_1 = 3Q_1 - 3Q_2 + Q_3 \qquad \text{(E18)}$$

$$\alpha_2 = \frac{8Q_2 - 5Q_1 - 3Q_3}{2\, \Delta x} \qquad \text{(E19)}$$

$$\alpha_3 = \frac{Q_3 - 2Q_2 + Q_1}{2\, \Delta x^2} \qquad \text{(E20)}$$

where

$$Q_0 = p(x_0, y) \qquad \text{(E21)}$$

$$Q_1 = \frac{p(x_0 + \Delta x, y) - p(x_0, y)}{\Delta x} \qquad \text{(E22)}$$

$$Q_2 = \frac{p(x_0 + 2\,\Delta x, y) - p(x_0, y)}{2\,\Delta x} \tag{E23}$$

$$Q_3 = \frac{p(x_0 + 3\,\Delta x, y) - p(x_0, y)}{3\,\Delta x} \tag{E24}$$

APPENDIX F

SAMPLE PROBLEMS

The appendix contains complete pressure and velocity printouts for four sample problems. These printouts can be used to debug and check computer programs.

Problem 1

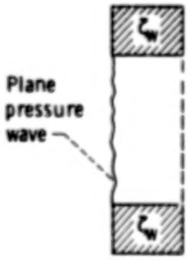

(a)

The input is

$\eta = 0.6$

$\eta^+ = 0$ (wave envelope concept not used)

$M = 0$

$L^*/H^* = 0.5$

$\zeta_w = 0.16 - i\,0.34$

$P(0, y) = 1$

$n = 5$

$m = 10$

The calculated values are

$$\Delta x = 0.1$$

$$\Delta y = 0.1111$$

$$E_0 = 1.30$$

$$E_x = 0.128 \ (x = 0.5)$$

$$\Delta dB = -10.04432$$

k	a_k		b_k		c_k		d_k		e_k	
1	-.123+01	.000	-.100+01	.000	.429+01	.000	-.196+01	.000	-.123+01	.000
2	-.123+01	.000	-.200+01	.000	.228+01	.949+00	.000	.000	-.123+01	.000
3	-.123+01	.000	.000	.000	.228+01	.949+00	-.200+01	.000	-.123+01	.000
4	-.247+01	.000	-.100+01	.000	.429+01	.931+00	-.100+01	.000	.000	.000
5	-.247+01	.000	-.200+01	.000	.228+01	.188+01	.000	.000	.000	.000
6	-.247+01	.000	.000	.000	.228+01	.188+01	-.200+01	.000	.000	.000

i	x position	j	|P|	j	|P|	j	|P|	j	|P|	j	|P|
1	.0000	1	.100+01	2	.100+01	3	.100+01	4	.100+01	5	.100+01
2	.1000+00	1	.178+01	2	.725+00	3	.793+00	4	.886+00	5	.926+00
3	.2000+00	1	.175+01	2	.516+00	3	.578+00	4	.717+00	5	.792+00
4	.3000+00	1	.793+00	2	.318+00	3	.393+00	4	.560+00	5	.650+00
5	.4000+00	1	.599+00	2	.169+00	3	.262+00	4	.446+00	5	.541+00
6	.5000+00	1	.598+00	2	.144+00	3	.213+00	4	.404+00	5	.500+00
1	.0000	6	.100+01	7	.100+01	8	.100+01	9	.100+01	10	.106+01
2	.1000+00	6	.926+00	7	.886+00	8	.793+00	9	.725+00	10	.108+01
3	.2000+00	6	.792+00	7	.717+00	8	.578+00	9	.518+00	10	.175+01
4	.3000+00	6	.650+00	7	.560+00	8	.393+00	9	.318+00	10	.793+00
5	.4000+00	6	.541+00	7	.446+00	8	.262+00	9	.169+00	10	.599+00
6	.5000+00	6	.500+00	7	.404+00	8	.213+00	9	.144+00	10	.598+00

i	x position	j	$p^{(1)}$	j	$p^{(1)}$	j	$p^{(1)}$	j	$p^{(1)}$	j	$p^{(1)}$
1	.0000	1	.100+01	2	.100+01	3	.100+01	4	.100+01	5	.100+01
2	.1000+00	1	.341+00	2	.574+00	3	.752+00	4	.860+00	5	.979+00
3	.2000+00	1	-.511+00	2	.111+00	3	.456+00	4	.644+00	5	.729+00
4	.3000+00	1	-.778+00	2	-.142+00	3	.216+00	4	.421+00	5	.515+00
5	.4000+00	1	-.477+00	2	-.146+00	3	.775-01	4	.229+00	5	.313+00
6	.5000+00	1	-.171+00	2	-.109+00	3	-.142-01	4	.670-01	5	.110+00
1	.0000	6	.100+01	7	.100+01	8	.100+01	9	.100+01	10	.100+01
2	.1000+00	6	.979+00	7	.860+00	8	.752+00	9	.574+00	10	.341+00
3	.2000+00	6	.729+00	7	[illegible]	8	.456+00	9	.111+00	10	-.511+00
4	.3000+00	6	.515+00	7	[illegible]	8	.216+00	9	-.142+00	10	-.156+00
5	.4000+00	6	.313+00	7	[illegible]	8	.775-01	9	-.146+00	10	-.477+00
6	.5000+00	6	.110+00	7	.670-01	8	-.142-01	9	-.109+00	10	-.171+00

i	x position	j	$p^{(2)}$	j	$p^{(2)}$	j	$p^{(2)}$	j	$p^{(2)}$	j	$p^{(2)}$
1	.0000	1	.000	2	.000	3	.000	4	.000	5	.000
2	.1000+00	1	-.173+01	2	-.443+00	3	-.250+00	4	-.190+00	5	-.174+00
3	.2000+00	1	-.916+00	2	-.576+00	3	-.358+00	4	-.316+00	5	-.310+00
4	.3000+00	1	-.274+00	2	-.285+00	3	-.377+00	4	-.370+00	5	-.396+00
5	.4000+00	1	.363+00	2	-.299-01	3	-.251+00	4	-.384+00	5	-.444+00
6	.5000+00	1	.594+00	2	.975-01	3	-.212+00	4	-.388+00	5	-.498+00
1	.0000	6	.000	7	.000	8	.000	9	.000	10	.000
2	.1000+00	6	-.174+00	7	-.196+00	8	-.250+00	9	-.443+00	10	-.173+01
3	.2000+00	6	-.310+00	7	-.316+00	8	-.358+00	9	-.576+00	10	-.916+00
4	.3000+00	6	-.396+00	7	-.376+00	8	-.327+00	9	-.265+00	10	-.274+00
5	.4000+00	6	-.444+00	7	-.384+00	8	-.281+00	9	-.299-01	10	.363+00
6	.5000+00	6	-.498+00	7	-.396+00	8	-.212+00	9	.975-01	10	.594+00

i	x position	j	$u^{(1)}$	j	$u^{(1)}$	j	$u^{(1)}$	j	$u^{(1)}$	j	$u^{(1)}$
1	.0000	1	.177+02	2	.677+01	3	.302+01	4	.277+01	5	.192+01
2	.1000+00	1	.492+01	2	.379+01	3	.279+01	4	.172+01	5	.163+01
3	.2000+00	1	-.499+01	2	-.176+01	3	.376+00	4	.891+00	5	.111+01
4	.3000+00	1	-.718+01	2	-.473+01	3	-.677+00	4	.275+00	5	.659+00
5	.4000+00	1	-.315+01	2	-.391+01	3	-.472+00	4	.160+00	5	.455+00
6	.5000+00	1	-.246+00	2	-.276+00	3	.545-01	4	.391+00	5	.440+00
1	.0000	6	.182+01	7	.277+01	8	.372+01	9	.677+01	10	.177+02
2	.1000+00	6	.143+01	7	.172+01	8	.279+01	9	.379+01	10	.492+01
3	.2000+00	6	.111+01	7	.891+00	8	.376+00	9	-.108+01	10	-.499+01
4	.3000+00	6	.659+00	7	.275+00	8	-.677+00	9	-.273+01	10	-.718+01
5	.4000+00	6	.455+00	7	.160+00	8	-.472+00	9	-.151+01	10	-.315+01
6	.5000+00	6	.440+00	7	.391+00	8	.545-01	9	-.276+00	10	-.246+00

i	x position	j	$u^{(2)}$	j	$u^{(2)}$	j	$u^{(2)}$	j	$u^{(2)}$	j	$u^{(2)}$
1	.0000	1	-.795+00	2	-.248+01	3	-.168+01	4	-.724+00	5	-.239+00
2	.1000+00	1	-.178+02	2	-.576+01	3	-.299+01	4	-.191+01	5	-.145+01
3	.2000+00	1	-.679+01	2	-.396+01	3	-.280+01	4	-.278+01	5	-.275+01
4	.3000+00	1	.670+00	2	-.176+01	3	-.191+01	4	-.211+01	5	-.217+01
5	.4000+00	1	.302+01	2	.393+00	3	-.105+01	4	-.176+01	5	-.282+01
6	.5000+00	1	.127+01	2	.744-01	3	-.479+00	4	-.152+01	5	-.185+01
1	.0000	6	-.239+00	7	-.724+00	8	-.168+01	9	-.248+01	10	-.795+00
2	.1000+00	6	-.145+01	7	-.191+01	8	-.299+01	9	-.520+01	10	-.178+02
3	.2000+00	6	-.275+01	7	-.278+01	8	-.280+01	9	-.380+01	10	-.679+01
4	.3000+00	6	-.217+01	7	-.211+01	8	-.191+01	9	-.178+01	10	.670+00
5	.4000+00	6	-.282+01	7	-.176+01	8	-.105+01	9	.393+00	10	.302+01
6	.5000+00	6	-.185+01	7	-.152+01	8	-.479+00	9	.744-01	10	.127+01

i	x position	j	$v^{(1)}$	j	$v^{(1)}$	j	$v^{(1)}$	j	$v^{(1)}$	j	$v^{(1)}$
1	.0000	1	.000	2	.000	3	.000	4	.000	5	.000
2	.1000+00	1	-.670+01	2	-.273+01	3	-.681+00	4	-.258+00	5	-.507-01
3	.2000+00	1	-.552+01	2	-.213+01	3	-.694+00	4	-.141+00	5	-.898-02
4	.3000+00	1	.560+00	2	.332+00	3	.399+00	4	.328+00	5	.176+00
5	.4000+00	1	.466+01	2	.251+01	3	.152+01	4	.864+00	5	.285+00
6	.5000+00	1	.553+01	2	.346+01	3	.215+01	4	.127+01	5	.397+00
1	.0000	6	.000	7	.000	8	.000	9	.000	10	.000
2	.1000+00	6	.507-01	7	.258+00	8	.681+00	9	.273+01	10	.620+01
3	.2000+00	6	.898-02	7	.141+00	8	.694+00	9	.213+01	10	.552+01
4	.3000+00	6	-.176+00	7	-.328+00	8	-.399+00	9	-.332+00	10	-.560+00
5	.4000+00	6	-.285+00	7	-.864+00	8	-.152+01	9	-.251+01	10	-.466+01
6	.5000+00	6	-.397+00	7	-.172+01	8	-.215+01	9	-.340+01	10	-.553+01

i	x position	j	$v^{(2)}$	j	$v^{(2)}$	j	$v^{(2)}$	j	$v^{(2)}$	j	$v^{(2)}$
1	.0000	1	.000	2	.000	3	.000	4	.000	5	.000
2	.1000+00	1	.224+01	2	.197+01	3	.129+01	4	.691+00	5	.217+00
3	.2000+00	1	.739+01	2	.490+01	3	.277+01	4	.119+01	5	.370+00
4	.3000+00	1	.715+01	2	.411+01	3	.262+01	4	.130+01	5	.410+00
5	.4000+00	1	.304+01	2	.253+01	3	.178+01	4	.103+01	5	.377+00
6	.5000+00	1	-.578+00	2	.799+00	3	.676+00	4	.591+00	5	.197+00
1	.0000	6	.000	7	.000	8	.000	9	.000	10	.000
2	.1000+00	6	-.217+00	7	-.691+00	8	-.129+01	9	-.197+01	10	-.224+01
3	.2000+00	6	-.370+00	7	-.119+01	8	-.277+01	9	-.490+01	10	-.739+01
4	.3000+00	6	-.410+00	7	-.130+01	8	-.262+01	9	-.411+01	10	-.715+01
5	.4000+00	6	-.337+00	7	-.103+01	8	-.178+01	9	-.253+01	10	-.304+01
6	.5000+00	6	-.157+00	7	-.591+00	8	-.676+00	9	-.799+00	10	.578+00

Problem 2

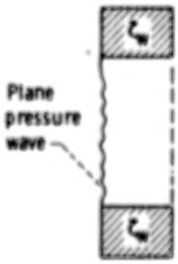

(b)

Problem 2 is the same as problem 1 except that the wave envelope concept is used. The input is

$$\eta = 0.6$$

$$\eta^{+} = 0.6$$

$$M = 0$$

$$L^{*}/H^{*} = 0.5$$

$$\zeta_{w} = 0.16 - i\,0.34$$

$$p(0, y) = 1$$

$$n = 5$$

$$m = 10$$

The calculated values are

$$\Delta x = 0.1$$

$$\Delta y = 0.1111$$

$$E_{0} = 1.21$$

$$E_{x} = 0.153 \ (x = 0.5)$$

$$\Delta dB = -9.01164$$

k	a_k		b_k		c_k		d_k		e_k	
1	-.123+01	-.465+00	-.100+01	.000	.447+01	.000	-.100+01	.000	-.123+01	.465+00
2	-.123+01	-.465+00	-.200+01	.000	.745+01	[illegible]	.000	.000	-.123+01	.465+00
3	-.123+01	-.465+00	.000	.000	.745+01	[illegible]	-.250+01	.000	-.123+01	.465+00
4	-.247+01	-.931+00	-.100+01	.000	.447+01	.931+00	-.100+01	.000	.000	.000
5	-.247+01	-.931+00	-.250+01	.000	.745+01	.188+01	.000	.000	.000	.000
6	-.247+01	-.931+00	.000	.000	.745+01	.188+01	-.250+01	.000	.000	.000

i	x position	j	|P|	j	|P|	j	|P|	j	|P|	j	|P|
1	.0000	1	.170+01	2	.170+01	3	.170+01	4	.100+01	5	.170+01
2	.1000+00	1	.110+01	2	.778+00	3	.798+00	4	.880+00	5	.973+00
3	.2000+00	1	.155+01	2	.673+00	3	.590+00	4	.772+00	5	.763+00
4	.3000+00	1	.798+00	2	.376+00	3	.478+00	4	.570+00	5	.677+00
5	.4000+00	1	.635+00	2	.187+00	3	.273+00	4	.466+00	5	.446+00
6	.5000+00	1	.621+00	2	.167+00	3	.226+00	4	.418+00	5	.536+00
1	.0000	6	.170+01	7	.170+01	8	.170+01	9	.170+01	10	.170+01
2	.1000+00	6	.972+00	7	.696+00	8	.798+00	9	.770+00	10	.112+01
3	.2000+00	6	.793+00	7	.772+00	8	.590+00	9	.578+00	10	.115+01
4	.3000+00	6	.657+00	7	.576+00	8	.478+00	9	.370+00	10	.770+00
5	.4000+00	6	.584+00	7	.496+00	8	.273+00	9	.167+00	10	.675+00
6	.5000+00	6	.516+00	7	.418+00	8	.276+00	9	.167+00	10	.571+00

i	x position	j	$p^{(1)}$	j	$p^{(1)}$	j	$p^{(1)}$	j	$p^{(1)}$	j	$p^{(1)}$
1	.0000	1	.170+01	2	.170+01	3	.170+01	4	.170+01	5	.170+01
2	.1000+00	1	.779+00	2	.712+00	3	.798+00	4	.470+00	5	.570+00
3	.2000+00	1	.334+00	2	.489+00	3	.598+00	4	.694+00	5	.771+00
4	.3000+00	1	-.889-01	2	.212+00	3	.473+00	4	.529+00	5	.590+00
5	.4000+00	1	-.470+00	2	.276-01	3	.270+00	4	.417+00	5	.494+00
6	.5000+00	1	-.541+00	2	-.571-01	3	.221+00	4	.779+00	5	.473+00
1	.0000	6	.170+01	7	.170+01	8	.170+01	9	.170+01	10	.170+01
2	.1000+00	6	.978+00	7	.876+00	8	.798+00	9	.712+00	10	.779+00
3	.2000+00	6	.751+00	7	.696+00	8	.598+00	9	.669+00	10	.370+00
4	.3000+00	6	.594+00	7	.579+00	8	.473+00	9	.712+00	10	-.160+00
5	.4000+00	6	.488+00	7	.417+00	8	.270+00	9	.236+01	10	-.407+00
6	.5000+00	6	.453+00	7	.376+00	8	.271+00	9	-.171+01	10	-.541+00

i	x position	j	$p^{(2)}$	j	$p^{(2)}$	j	$p^{(2)}$	j	$p^{(2)}$	j	$p^{(2)}$
1	.0000	1	.000	2	.000	3	.000	4	.000	5	.000
2	.1000+00	1	-.818+00	2	-.176+00	3	.413-01	4	.172+00	5	.172+00
3	.2000+00	1	-.171+01	2	-.487+00	3	.470-01	4	.197+00	5	.257+00
4	.3000+00	1	-.793+00	2	-.413+00	3	.470-01	4	.210+00	5	.210+00
5	.4000+00	1	-.490+00	2	-.196+00	3	.447-01	4	.191+00	5	.272+00
6	.5000+00	1	-.361+00	2	-.179+00	3	.390-01	4	.170+00	5	.267+00
1	.0000	6	.000	7	.000	8	.000	9	.000	10	.000
2	.1000+00	6	.167+00	7	.172+00	8	.417-01	9	-.198+00	10	-.818+00
3	.2000+00	6	.287+00	7	.198+00	8	.470-01	9	-.267+00	10	-.171+01
4	.3000+00	6	.290+00	7	.276+00	8	.490-01	9	-.253+00	10	-.792+00
5	.4000+00	6	.282+00	7	.191+00	8	.443-01	9	-.186+00	10	-.491+00
6	.5000+00	6	.207+00	7	.178+00	8	.377-01	9	-.159+00	10	-.361+00

i	x position	j	$u_a^{(1)}$	j	$u_a^{(1)}$	j	$u_a^{(1)}$	j	$u_a^{(1)}$	j	$u_a^{(1)}$
1	.0000	1	.156+02	2	.570+01	3	.296+01	4	.270+01	5	.177+01
2	.1000+00	1	.799+01	2	.470+01	3	.299+01	4	.232+01	5	.710+01
3	.2000+00	1	.576+01	2	.102+01	3	.271+01	4	.226+01	5	.277+01
4	.3000+00	1	-.300+01	2	.103+00	3	.153+01	4	.270+01	5	.776+01
5	.4000+00	1	-.389+01	2	-.171+00	3	.171+01	4	.161+01	5	.276+01
6	.5000+00	1	-.172+01	2	-.780-01	3	.260+00	4	.190+01	5	.190+01
1	.0000	6	.197+01	7	.270+01	8	.256+01	9	.580+01	10	.156+02
2	.1000+00	6	.278+01	7	.272+01	8	.299+01	9	.470+01	10	.790+01
3	.2000+00	6	.227+01	7	.276+01	8	.221+01	9	.197+01	10	.576+01
4	.3000+00	6	.278+01	7	.278+01	8	.153+01	9	.153+01	10	-.260+01
5	.4000+00	6	.276+01	7	.191+01	8	.171+01	9	-.151+01	10	-.389+01
6	.5000+00	6	.156+01	7	.178+01	8	.408+00	9	-.767+01	10	-.172+01

i	x position	j	$u_a^{(2)}$	j	$u_a^{(2)}$	j	$u_a^{(2)}$	j	$u_a^{(2)}$	j	$u_a^{(2)}$
1	.0000	1	-.974+00	2	-.378+01	3	-.199+01	4	-.733+00	5	-.316+00
2	.1000+00	1	-.756+01	2	-.352+01	3	-.197+01	4	-.113+01	5	-.772+00
3	.2000+00	1	-.977+01	2	-.366+01	3	-.185+01	4	-.100+01	5	-.700+00
4	.3000+00	1	-.686+01	2	-.315+01	3	-.188+01	4	-.667+00	5	-.312+00
5	.4000+00	1	-.402+01	2	.271+01	3	-.611+00	4	-.410+00	5	.370+00
6	.5000+00	1	-.178+01	2	-.496+00	3	.198+00	4	.470+00	5	.918+00
1	.0000	6	-.316+00	7	-.673+00	8	-.198+01	9	-.375+01	10	-.470+00
2	.1000+00	6	-.772+00	7	-.113+01	8	-.197+01	9	-.352+01	10	-.756+01
3	.2000+00	6	-.700+00	7	-.176+01	8	-.185+01	9	-.367+01	10	-.977+01
4	.3000+00	6	-.312+00	7	-.667+00	8	-.188+01	9	-.315+01	10	-.686+01
5	.4000+00	6	.370+00	7	-.415+01	8	-.611+00	9	-.271+01	10	-.402+01
6	.5000+00	6	.918+00	7	.670+00	8	.176+00	9	-.496+00	10	-.178+01

i	x position	j	$v_a^{(1)}$	j	$v_a^{(1)}$	j	$v_a^{(1)}$	j	$v_a^{(1)}$	j	$v_a^{(1)}$
1	.0000	1	.000	2	.000	3	.000	4	.000	5	.000
2	.1000+00	1	-.678+01	2	-.318+01	3	-.173+01	4	-.461+00	5	-.117+00
3	.2000+00	1	-.912+01	2	-.470+01	3	-.196+01	4	-.858+00	5	-.241+00
4	.3000+00	1	-.674+01	2	-.355+01	3	-.197+01	4	-.962+00	5	-.371+00
5	.4000+00	1	-.370+01	2	-.247+01	3	-.170+01	4	-.970+00	5	-.313+00
6	.5000+00	1	-.158+01	2	-.199+01	3	-.156+01	4	-.985+00	5	-.312+00
1	.0000	6	.000	7	.000	8	.000	9	.000	10	.000
2	.1000+00	6	.117+00	7	.461+00	8	.173+01	9	.318+01	10	.678+01
3	.2000+00	6	.241+00	7	.878+00	8	.196+01	9	.420+01	10	.912+01
4	.3000+00	6	.301+00	7	.962+00	8	.197+01	9	.355+01	10	.674+01
5	.4000+00	6	.313+00	7	.970+00	8	.170+01	9	.247+01	10	.370+01
6	.5000+00	6	.312+00	7	.985+00	8	.156+01	9	.199+01	10	.158+01

i	x position	j	$v_a^{(2)}$	j	$v_a^{(2)}$	j	$v_a^{(2)}$	j	$v_a^{(2)}$	j	$v_a^{(2)}$
1	.0000	1	.000	2	.000	3	.000	4	.000	5	.000
2	.1000+00	1	-.118+01	2	.719+00	3	.616+00	4	.517+00	5	.173+00
3	.2000+00	1	.172+01	2	.173+01	3	.118+01	4	.766+00	5	.258+00
4	.3000+00	1	.179+01	2	.202+01	3	.179+01	4	.862+00	5	.296+00
5	.4000+00	1	.575+01	2	.277+01	3	.166+01	4	.962+00	5	.317+00
6	.5000+00	1	[illegible]	2	.316+01	3	.196+01	4	.171+01	5	.376+00
1	.0000	6	.000	7	.000	8	.000	9	.000	10	.000
2	.1000+00	6	-.173+00	7	-.517+00	8	-.616+00	9	-.719+00	10	.118+01
3	.2000+00	6	-.258+00	7	-.766+00	8	-.118+01	9	-.133+01	10	-.172+01
4	.3000+00	6	-.296+00	7	-.862+00	8	-.178+01	9	-.202+01	10	-.179+01
5	.4000+00	6	-.317+00	7	-.962+00	8	-.169+01	9	-.277+01	10	-.575+01
6	.5000+00	6	-.376+00	7	-.171+01	8	-.196+01	9	-.316+01	10	-.579+01

Problem 3

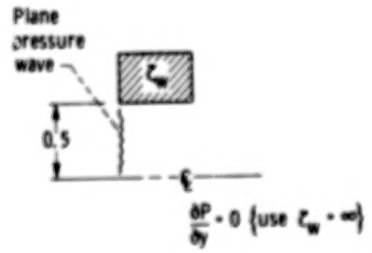

(c)

The input is

$\eta = 0.6$

$\eta^+ = 0$ (wave envelope concept not used)

$M = 0.5$

$\zeta_w = 0.071 - 0.151$ (upper)

$\zeta_w = 1\times10^{30}$ (centerline)

$P(0, y) = 1$

$n = 10$

$m = 10$

The calculated values are

$$\Delta x = 0.05$$

$$\Delta y = 0.05556$$

$$E_0 = 2.64$$

$$E_x = 0.725 \ (x = 0.5)$$

$$\Delta dB = -5.60602$$

k	a_k		b_k		c_k		d_k		e_k	
1	-.926+00	-.116+00	-.150+01	.000	.781+01	.000	-.170+01	.000	-.826+00	.116+00
2	.122+02	-.137+02	-.200+01	.000	-.708+02	.161+02	.000	.000	.170+02	-.137+01
3	-.926+00	-.116+00	.000	.000	.781+01	.316+00	-.250+01	.000	-.926+00	.116+00
4	-.185+01	-.233+00	-.100+01	-.796+01	.781+01	.160+02	-.150+01	-.796+01	.000	.000
5	.282+02	-.193+02	-.200+01	-.159+02	-.735+02	.761+02	.376	.000	.000	.000
6	-.185+01	-.233+00	.000	.000	.781+01	.160+02	-.276+01	-.159+02	.000	.000

i	x position	j	|P|	j	|P|	j	|P|	j	|P|	j	|P|
1	.0000	1	.100+01	2	.100+01	3	.100+01	4	.100+01	5	.100+01
2	.5000-01	1	.952+00	2	.951+00	3	.949+00	4	.945+00	5	.941+00
3	.1000+00	1	.857+00	2	.856+00	3	.852+00	4	.847+00	5	.843+00
4	.1500+00	1	.725+00	2	.723+00	3	.719+00	4	.715+00	5	.715+00
5	.2000+00	1	.567+00	2	.566+00	3	.563+00	4	.563+00	5	.571+00
6	.2500+00	1	.405+00	2	.405+00	3	.406+00	4	.414+00	5	.439+00
7	.3000+00	1	.279+00	2	.282+00	3	.292+00	4	.316+00	5	.360+00
8	.3500+00	1	.263+00	2	.259+00	3	.289+00	4	.327+00	5	.394+00
9	.4000+00	1	.341+00	2	.348+00	3	.392+00	4	.472+00	5	.456+00
10	.4500+00	1	.448+00	2	.456+00	3	.490+00	4	.532+00	5	.564+00
11	.5000+00	1	.541+00	2	.549+00	3	.574+00	4	.617+00	5	.679+00
1	.0000	6	.100+01	7	.100+01	8	.100+01	9	.100+01	10	.100+01
2	.5000-01	6	.978+00	7	.979+00	8	.966+00	9	.961+00	10	.995+00
3	.1000+00	6	.888+00	7	.896+00	8	.883+00	9	.931+00	10	.100+01
4	.1500+00	6	.776+00	7	.777+00	8	.816+00	9	.910+00	10	.106+01
5	.2000+00	6	.599+00	7	.646+00	8	.783+00	9	.899+00	10	.110+01
6	.2500+00	6	.488+00	7	.575+00	8	.709+00	9	.890+00	10	.116+01
7	.3000+00	6	.474+00	7	.566+00	8	.699+00	9	.913+00	10	.121+01
8	.3500+00	6	.486+00	7	.576+00	8	.720+00	9	.960+00	10	.124+01
9	.4000+00	6	.559+00	7	.681+00	8	.795+00	9	.970+00	10	.125+01
10	.4500+00	6	.667+00	7	.762+00	8	.878+00	9	.103+01	10	.124+01
11	.5000+00	6	.740+00	7	.859+00	8	.973+00	9	.109+01	10	.126+01

i	x position	j	$P^{(1)}$	j	$P^{(1)}$	j	$P^{(1)}$	j	$P^{(1)}$	j	$P^{(1)}$
1	.0000	1	.100+01	2	.100+01	3	.100+01	4	.100+01	5	.100+01
2	.5000-01	1	.952+00	2	.951+00	3	.948+00	4	.945+00	5	.941+00
3	.1000+00	1	.857+00	2	.856+00	3	.852+00	4	.847+00	5	.842+00
4	.1500+00	1	.724+00	2	.723+00	3	.719+00	4	.714+00	5	.710+00
5	.2000+00	1	.567+00	2	.565+00	3	.561+00	4	.556+00	5	.552+00
6	.2500+00	1	.398+00	2	.386+00	3	.381+00	4	.384+00	5	.378+00
7	.3000+00	1	.271+00	2	.279+00	3	.271+00	4	.211+00	5	.270+00
8	.3500+00	1	.613-01	2	.776-01	3	.158-01	4	.494-01	5	.299-01
9	.4000+00	1	-.401-01	2	-.487-01	3	-.477-01	4	-.402-01	5	-.123+00
10	.4500+00	1	-.174+00	2	-.171+00	3	-.184+00	4	-.191+00	5	-.242+00
11	.5000+00	1	-.166+00	2	-.174+00	3	-.202+00	4	-.251+00	5	-.319+00
1	.0000	6	.100+01	7	.100+01	8	.100+01	9	.100+01	10	.100+01
2	.5000-01	6	.978+00	7	.977+00	8	.960+00	9	.951+00	10	.988+00
3	.1000+00	6	.879+00	7	.863+00	8	.878+00	9	.886+00	10	.973+00
4	.1500+00	6	.710+00	7	.719+00	8	.760+00	9	.790+00	10	.871+00
5	.2000+00	6	.584+00	7	.547+00	8	.677+00	9	.666+00	10	.796+00
6	.2500+00	6	.372+00	7	.396+00	8	.592+00	9	.484+00	10	.616+00
7	.3000+00	6	.193+00	7	.194+00	8	.112+00	9	.262+00	10	.376+00
8	.3500+00	6	.799-02	7	-.897-02	8	-.172-01	9	-.496-02	10	.271-01
9	.4000+00	6	-.143+00	7	-.287+00	8	-.181+00	9	-.207+00	10	-.373+00
10	.4500+00	6	-.317+00	7	-.383+00	8	-.270+00	9	-.371+00	10	-.373+00
11	.5000+00	6	-.410+00	7	-.573+00	8	-.177+00	9	-.480+00	10	-.484+00

i	x position	j	$p^{(2)}$	j	$p^{(2)}$	j	$p^{(2)}$	j	$p^{(2)}$	j	$p^{(2)}$
1	.0000	1	.000	2	.000	3	.000	4	.000	5	.000
2	.5000-01	1	.271-01	2	.198-01	3	.178-01	4	.906-02	5	-.164-01
3	.1000+00	1	.351-01	2	.256-01	3	.118-01	4	-.117-01	5	-.457-01
4	.1500+00	1	.178-01	2	.114-01	3	-.649-02	4	-.414-01	5	-.897-01
5	.2000+00	1	-.179-01	2	-.256-01	3	-.492-01	4	-.897-01	5	-.148+00
6	.2500+00	1	-.770-01	2	-.854-01	3	-.111+00	4	-.155+00	5	-.220+00
7	.3000+00	1	-.156+00	2	-.165+00	3	-.191+00	4	-.235+00	5	-.300+00
8	.3500+00	1	-.250+00	2	-.258+00	3	-.282+00	4	-.323+00	5	-.383+00
9	.4000+00	1	-.348+00	2	-.355+00	3	-.377+00	4	-.413+00	5	-.465+00
10	.4500+00	1	-.441+00	2	-.447+00	3	-.466+00	4	-.496+00	5	-.536+00
11	.5000+00	1	-.515+00	2	-.521+00	3	-.537+00	4	-.564+00	5	-.599+00
1	.0000	6	.000	7	.000	8	.000	9	.000	10	.000
2	.5000-01	6	-.395-01	7	-.695-01	8	-.103+00	9	-.142+00	10	-.182+00
3	.1000+00	6	-.989-01	7	-.146+00	8	-.215+00	9	-.288+00	10	-.362+00
4	.1500+00	6	-.156+00	7	-.216+00	8	-.336+00	9	-.444+00	10	-.557+00
5	.2000+00	6	-.278+00	7	-.329+00	8	-.455+00	9	-.600+00	10	-.771+00
6	.2500+00	6	-.358+00	7	-.423+00	8	-.570+00	9	-.765+00	10	-.982+00
7	.3000+00	6	-.399+00	7	-.508+00	8	-.686+00	9	-.875+00	10	-.116+01
8	.3500+00	6	-.466+00	7	-.578+00	8	-.770+00	9	-.960+00	10	-.124+01
9	.4000+00	6	-.535+00	7	-.678+00	8	-.794+00	9	-.932+00	10	-.126+01
10	.4500+00	6	-.592+00	7	-.679+00	8	-.762+00	9	-.853+00	10	-.172+01
11	.5000+00	6	-.640+00	7	-.692+00	8	-.717+00	9	-.735+00	10	-.771+00

i	x position	j	$u^{(1)}$	j	$u^{(1)}$	j	$u^{(1)}$	j	$u^{(1)}$	j	$u^{(1)}$
1	.0000	1	.287+01	2	.287+01	3	.296+01	4	.368+01	5	.479+01
2	.5000-01	1	.262+01	2	.256+01	3	.276+01	4	.321+01	5	.390+01
3	.1000+00	1	.223+01	2	.270+01	3	.269+01	4	.292+01	5	.372+01
4	.1500+00	1	.272+01	2	.275+01	3	.217+01	4	.236+01	5	.293+01
5	.2000+00	1	.177+01	2	.176+01	3	.192+01	4	.186+01	5	.190+01
6	.2500+00	1	.149+01	2	.148+01	3	.165+01	4	.177+01	5	.176+01
7	.3000+00	1	.119+01	2	.116+01	3	.127+01	4	.692+00	5	.591+00
8	.3500+00	1	.321+00	2	.792+00	3	.676+00	4	.663+00	5	.775+00
9	.4000+00	1	.470+00	2	.377+00	3	.265+00	4	.592-02	5	-.376+00
10	.4500+00	1	-.6 7-01	2	.172+00	3	-.277+00	4	-.667+00	5	-.778+00
11	.5000+00	1	-.619+00	2	-.684+00	3	-.742+00	4	-.944+00	5	-.170+01
1	.0000	6	.566+01	7	.771+01	8	.970+01	9	.133+02	10	.185+02
2	.5000-01	6	.699+01	7	.679+01	8	.925+01	9	.110+02	10	.180+02
3	.1000+00	6	.470+01	7	.692+01	8	.613+01	9	.773+01	10	.986+01
4	.1500+00	6	.295+01	7	.132+01	8	.369+01	9	.396+01	10	.470+01
5	.2000+00	6	.197+01	7	.172+01	8	.130+01	9	.363+00	10	-.170+01
6	.2500+00	6	.696+00	7	.327+00	8	-.648+00	9	-.264+01	10	-.565+01
7	.3000+00	6	.423-01	7	-.772+00	8	-.275+01	9	-.621+01	10	-.790+01
8	.3500+00	6	-.576+00	7	-.179+01	8	-.273+01	9	-.677+01	10	-.770+01
9	.4000+00	6	-.970+00	7	-.176+01	8	-.288+01	9	-.665+01	10	-.684+01
10	.4500+00	6	-.175+01	7	-.189+01	8	-.272+01	9	-.378+01	10	-.475+01
11	.5000+00	6	-.155+01	7	-.187+01	8	-.288+01	9	-.390+01	10	-.383+01

i	x position	j	$u^{(2)}$	j	$u^{(2)}$	j	$u^{(2)}$	j	$u^{(2)}$	j	$u^{(2)}$
1	.0000	1	-.672+00	2	-.686+00	3	[illegible]	4	-.117+01	5	-.194+01
2	.5000-01	1	-.191+01	2	-.197+01	3	[illegible]	4	-.266+01	5	-.291+01
3	.1000+00	1	-.295+01	2	-.291+01	3	[illegible]	4	-.366+01	5	-.476+01
4	.1500+00	1	-.356+01	2	-.363+01	3	-.395+01	4	-.426+01	5	-.441+01
5	.2000+00	1	-.470+01	2	-.477+01	3	-.479+01	4	-.467+01	5	-.576+01
6	.2500+00	1	-.418+01	2	-.420+01	3	[illegible]	4	-.470+01	5	[illegible]
7	.3000+00	1	-.470+01	2	-.414+01	3	-.471+01	4	-.461+01	5	-.570+01
8	.3500+00	1	-.376+01	2	-.371+01	3	-.395+01	4	-.427+01	5	-.473+01
9	.4000+00	1	-.375+01	2	-.379+01	3	-.361+01	4	-.360+01	5	-.396+01
10	.4500+00	1	-.262+01	2	-.266+01	3	-.275+01	4	-.209+01	5	-.376+01
11	.5000+00	1	-.194+01	2	-.196+01	3	-.272+01	4	-.212+01	5	-.276+01
1	.0000	6	-.196+01	7	-.265+01	8	-.366+01	9	-.516+01	10	-.766+01
2	.5000-01	6	-.303+01	7	-.476+01	8	-.679+01	9	-.972+01	10	-.126+02
3	.1000+00	6	-.493+01	7	-.672+01	8	-.818+01	9	-.112+02	10	-.148+02
4	.1500+00	6	-.576+01	7	-.712+01	8	-.916+01	9	-.172+02	10	-.173+02
5	.2000+00	6	-.612+01	7	-.726+01	8	-.916+01	9	-.119+02	10	-.184+02
6	.2500+00	6	-.673+01	7	-.773+01	8	-.639+01	9	-.102+02	10	-.170+02
7	.3000+00	6	-.549+01	7	-.676+01	8	-.713+01	9	-.902+01	10	-.899+01
8	.3500+00	6	-.493+01	7	-.576+01	8	-.572+01	9	-.581+01	10	-.571+01
9	.4000+00	6	-.414+01	7	-.479+01	8	-.467+01	9	-.411+01	10	-.276+01
10	.4500+00	6	-.379+01	7	-.347+01	8	-.349+01	9	-.316+01	10	-.276+01
11	.5000+00	6	-.241+01	7	-.287+01	8	-.276+01	9	-.277+01	10	-.277+01

i	x position	j	$v^{(1)}$	j	$v^{(1)}$	j	$v^{(1)}$	j	$v^{(1)}$	j	$v^{(1)}$
1	.0000	1	-.159-02	2	.190+00	3	.393+00	4	.621+00	5	.976+00
2	.5000-01	1	-.279-02	2	.390+00	3	.721+00	4	.117+01	5	.175+01
3	.1000+00	1	-.276-02	2	.472+00	3	.497+00	4	.161+01	5	.279+01
4	.1500+00	1	-.284-02	2	.564+00	3	.118+01	4	.190+01	5	.279+01
5	.2000+00	1	-.275-02	2	.611+00	3	.177+01	4	.272+01	5	.293+01
6	.2500+00	1	-.115-02	2	.614+00	3	.177+01	4	.190+01	5	.293+01
7	.3000+00	1	-.179-03	2	.590+00	3	.118+01	4	.193+01	5	.255+01
8	.3500+00	1	.662-03	2	.576+00	3	.175+01	4	.190+01	5	.217+01
9	.4000+00	1	.170-02	2	.446+00	3	.887+00	4	.133+01	5	.175+01
10	.4500+00	1	.145-02	2	.371+00	3	.798+00	4	.176+01	5	.176+01
11	.5000+00	1	.149-02	2	.372+00	3	.595+00	4	.982+00	5	.174+01
1	.0000	6	.135+01	7	.197+01	8	.291+01	9	.435+01	10	.666+01
2	.5000-01	6	.256+01	7	.386+01	8	.571+01	9	.796+01	10	.116+02
3	.1000+00	6	.343+01	7	.499+01	8	.690+01	9	.101+02	10	.144+02
4	.1500+00	6	.398+01	7	.553+01	8	.777+01	9	.110+02	10	.160+02
5	.2000+00	6	.407+01	7	.550+01	8	.763+01	9	.106+02	10	.147+02
6	.2500+00	6	.398+01	7	.511+01	8	.672+01	9	.883+01	10	.117+02
7	.3000+00	6	.337+01	7	.470+01	8	.535+01	9	.650+01	10	.767+01
8	.3500+00	6	.275+01	7	.373+01	8	.384+01	9	.412+01	10	.381+01
9	.4000+00	6	.212+01	7	.260+01	8	.288+01	9	.216+01	10	.995+00
10	.4500+00	6	.157+01	7	.143+01	8	.145+01	9	.957+00	10	-.445+00
11	.5000+00	6	.115+01	7	.159+01	8	.795+00	9	.179+00	10	-.971+00

I	x position	J	$v_a^{(2)}$	J	$v_a^{(2)}$	J	$v_a^{(2)}$	J	$v_a^{(2)}$	J	$v_a^{(2)}$
1	.0000	1	-.235-02	2	.369+00	3	.790+00	4	.130+01	5	.197+01
2	.5000-01	1	-.218-02	2	.355+00	3	.761+00	4	.126+01	5	.190+01
3	.1000+00	1	-.182-02	2	.342+00	3	.731+00	4	.120+01	5	.182+01
4	.1500+00	1	-.128-02	2	.329+00	3	.699+00	4	.114+01	5	.171+01
5	.2000+00	1	-.622-03	2	.313+00	3	.658+00	4	.106+01	5	.156+01
6	.2500+00	1	.496-04	2	.292+00	3	.606+00	4	.963+00	5	.139+01
7	.3000+00	1	.619-03	2	.266+00	3	.542+00	4	.845+00	5	.118+01
8	.3500+00	1	.101-02	2	.236+00	3	.473+00	4	.719+00	5	.969+00
9	.4000+00	1	.174-02	2	.208+00	3	.410+00	4	.605+00	5	.779+00
10	.4500+00	1	.138-02	2	.190+00	3	.367+00	4	.526+00	5	.646+00
11	.5000+00	1	.145-02	2	.183+00	3	.352+00	4	.498+00	5	.596+00
1	.0000	6	.289+01	7	.419+01	8	.607+01	9	.882+01	10	.179+02
2	.5000-01	6	.279+01	7	.405+01	8	.587+01	9	.853+01	10	.126+02
3	.1000+00	6	.265+01	7	.381+01	8	.548+01	9	.792+01	10	.116+02
4	.1500+00	6	.245+01	7	.347+01	8	.489+01	9	.692+01	10	.996+01
5	.2000+00	6	.220+01	7	.303+01	8	.411+01	9	.557+01	10	.759+01
6	.2500+00	6	.189+01	7	.250+01	8	.321+01	9	.400+01	10	.484+01
7	.3000+00	6	.155+01	7	.193+01	8	.227+01	9	.243+01	10	.213+01
8	.3500+00	6	.120+01	7	.138+01	8	.141+01	9	.109+01	10	-.693-01
9	.4000+00	6	.901+00	7	.916+00	8	.720+00	9	.978-01	10	-.142+01
10	.4500+00	6	.689+00	7	.597+00	8	.270+00	9	-.450+00	10	-.187+01
11	.5000+00	6	.611+00	7	.477+00	8	.196+00	9	-.616+00	10	-.192+01

Problem 4

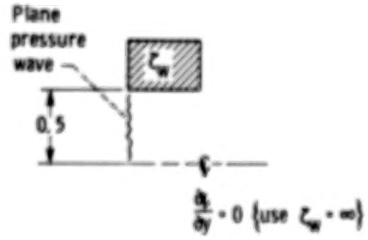

(d)

$\eta = 0.6$

$\eta^+ = 0.6$

$M = 0.5$

$\zeta_w = 0.071 - 0.151$ (upper)

$\zeta_w = 1 \times 10^{30}$ (centerline)

$p(0, y) = 1$

$n = 10$

$m = 10$

The calculated values are

$$\Delta x = 0.5$$

$$\Delta y = 0.05556$$

$$E_0 = 2.18$$

$$E_x = 0.853 \ (x = 0.5)$$

$$\Delta dB = -4.07234$$

k	a_k		b_k		c_k		d_k		e_k	
1	-.926+00	-.233+00	-.100+01	.000	.385+01	.000	-.100+01	.000	-.926+00	.233+00
2	.132+02	-.116+02	-.200+01	.000	-.291+02	.155+02	.000	.000	.169+02	-.327+01
3	-.926+00	-.233+00	.000	.000	.385+01	.304-29	-.200+01	.000	-.926+00	.233+00
4	-.185+01	-.465+00	-.100+01	-.796+01	.385+01	.164+02	-.100+01	-.796+01	.000	.000
5	.282+02	-.195+02	-.200+01	-.159+02	-.310+02	.279+02	.000	.000	.000	.000
6	-.185+01	-.465+00	.000	.000	.385+01	.164+02	-.200+01	-.159+02	.000	.000

i	x position	j	$\|P\|$	j	$\|P\|$	j	$\|P\|$	j	$\|P\|$	j	$\|P\|$
1	.0000	1	.100+01	2	.100+01	3	.100+01	4	.100+01	5	.100+01
2	.5000-01	1	.942+00	2	.941+00	3	.940+00	4	.937+00	5	.935+00
3	.1000+00	1	.843+00	2	.843+00	3	.840+00	4	.838+00	5	.836+00
4	.1500+00	1	.715+00	2	.714+00	3	.713+00	4	.712+00	5	.716+00
5	.2000+00	1	.572+00	2	.572+00	3	.573+00	4	.578+00	5	.590+00
6	.2500+00	1	.441+00	2	.443+00	3	.448+00	4	.461+00	5	.487+00
7	.3000+00	1	.366+00	2	.370+00	3	.382+00	4	.405+00	5	.444+00
8	.3500+00	1	.384+00	2	.389+00	3	.406+00	4	.436+00	5	.482+00
9	.4000+00	1	.466+00	2	.473+00	3	.492+00	4	.526+00	5	.574+00
10	.4500+00	1	.560+00	2	.567+00	3	.589+00	4	.625+00	5	.676+00
11	.5600+00	1	.632+00	2	.640+00	3	.663+00	4	.702+00	5	.758+00
1	.0000	6	.100+01	7	.100+01	8	.100+01	9	.100+01	10	.100+01
2	.5000-01	6	.932+00	7	.932+00	8	.933+00	9	.936+00	10	.940+00
3	.1000+00	6	.878+00	7	.845+00	8	.860+00	9	.883+00	10	.910+00
4	.1500+00	6	.727+00	7	.750+00	8	.790+00	9	.848+00	10	.916+00
5	.2000+00	6	.616+00	7	.662+00	8	.734+00	9	.833+00	10	.956+00
6	.2500+00	6	.531+00	7	.601+00	8	.703+00	9	.841+00	10	.102+01
7	.3000+00	6	.504+00	7	.589+00	8	.708+00	9	.870+00	10	.109+01
8	.3500+00	6	.547+00	7	.634+00	8	.753+00	9	.918+00	10	.116+01
9	.4000+00	6	.638+00	7	.721+00	8	.830+00	9	.981+00	10	.121+01
10	.4500+00	6	.743+00	7	.825+00	8	.927+00	9	.106+01	10	.125+01
11	.5000+00	6	.832+00	7	.924+00	8	.103+01	9	.115+01	10	.125+01

i	x position	j	$p^{(1)}$	j	$p^{(1)}$	j	$p^{(1)}$	j	$p^{(1)}$	j	$p^{(1)}$
1	.0000	1	.100+01	2	.100+01	3	.100+01	4	.100+01	5	.100+01
2	.5000-01	1	.934+00	2	.934+00	3	.933+00	4	.931+00	5	.930+00
3	.1000+00	1	.820+00	2	.820+00	3	.820+00	4	.821+00	5	.824+00
4	.1500+00	1	.690+00	2	.691+00	3	.694+00	4	.690+00	5	.701+00
5	.2000+00	1	.542+00	2	.544+00	3	.550+00	4	.562+00	5	.583+00
6	.2500+00	1	.431+00	2	.433+00	3	.442+00	4	.459+00	5	.487+00
7	.3000+00	1	.365+00	2	.366+00	3	.379+00	4	.397+00	5	.428+00
8	.3500+00	1	.354+00	2	.357+00	3	.367+00	4	.385+00	5	.414+00
9	.4000+00	1	.393+00	2	.396+00	3	.405+00	4	.421+00	5	.445+00
10	.4500+00	1	.467+00	2	.470+00	3	.479+00	4	.493+00	5	.513+00
11	.5000+00	1	.550+00	2	.553+00	3	.563+00	4	.579+00	5	.600+00
1	.0000	6	.100+01	7	.100+01	8	.100+01	9	.100+01	10	.100+01
2	.5000-01	6	.930+00	7	.930+00	8	.932+00	9	.935+00	10	.937+00
3	.1000+00	6	.871+00	7	.842+00	8	.859+00	9	.882+00	10	.904+00
4	.1500+00	6	.720+00	7	.749+00	8	.790+00	9	.884+00	10	.956+00
5	.2000+00	6	.615+00	7	.662+00	8	.730+00	9	.822+00	10	.939+00
6	.2500+00	6	.529+00	7	.592+00	8	.683+00	9	.811+00	10	.986+00
7	.3000+00	6	.475+00	7	.545+00	8	.648+00	9	.800+00	10	.102+01
8	.3500+00	6	.458+00	7	.524+00	8	.624+00	9	.778+00	10	.102+01
9	.4000+00	6	.481+00	7	.533+00	8	.612+00	9	.739+00	10	.952+00
10	.4500+00	6	.539+00	7	.572+00	8	.617+00	9	.685+00	10	.810+00
11	.5000+00	6	.622+00	7	.643+00	8	.655+00	9	.646+00	10	.683+00

i	x position	j	$p^{(2)}$	j	$p^{(2)}$	j	$p^{(2)}$	j	$p^{(2)}$	j	$p^{(2)}$
1	.0000	1	.000	2	.000	3	.000	4	.000	5	.000
2	.5000-01	1	.120+00	2	.118+00	3	.113+00	4	.103+00	5	.902-01
3	.1000+00	1	.199+00	2	.195+00	3	.184+00	4	.166+00	5	.141+00
4	.1500+00	1	.221+00	2	.216+00	3	.201+00	4	.177+00	5	.142+00
5	.2000+00	1	.184+00	2	.178+00	3	.161+00	4	.133+00	5	.935-01
6	.2500+00	1	.960-01	2	.699-01	3	.719-01	4	.422-01	5	.165-02
7	.3000+00	1	-.228-01	2	-.291-01	3	-.476-01	4	-.778-01	5	-.119+00
8	.3500+00	1	-.147+00	2	-.154+00	3	-.173+00	4	-.205+00	5	-.247+00
9	.4000+00	1	-.251+00	2	-.258+00	3	-.279+00	4	-.314+00	5	-.362+00
10	.4500+00	1	-.310+00	2	-.318+00	3	-.343+00	4	-.384+00	5	-.440+00
11	.5000+00	1	-.312+00	2	-.321+00	3	-.349+00	4	-.396+00	5	-.464+00
1	.0000	6	.000	7	.000	8	.000	9	.000	10	.000
2	.5000-01	6	.725-01	7	.502-01	8	.225-01	9	-.131-01	10	-.653-01
3	.1000+00	6	.108+00	7	.666-01	8	.180-01	9	-.380-01	10	-.103+00
4	.1500+00	6	.983-01	7	.455-01	8	-.141-01	9	-.763-01	10	-.132+00
5	.2000+00	6	.443-01	7	-.134-01	8	-.761-01	9	-.136+00	10	-.177+00
6	.2500+00	6	-.486-01	7	-.106+00	8	-.168+00	9	-.224+00	10	-.258+00
7	.3000+00	6	-.168+00	7	-.225+00	8	-.286+00	9	-.343+00	10	-.395+00
8	.3500+00	6	-.299+00	7	-.357+00	8	-.471+00	9	-.488+00	10	-.557+00
9	.4000+00	6	-.420+00	7	-.486+00	8	-.561+00	9	-.646+00	10	-.754+00
10	.4500+00	6	-.511+00	7	-.595+00	8	-.692+00	9	-.802+00	10	-.946+00
11	.5000+00	6	-.553+00	7	-.663+00	8	-.796+00	9	-.946+00	10	-.110+01

i	x position	j	$u_a^{(1)}$	j	$u_a^{(1)}$	j	$u_a^{(1)}$	j	$u_a^{(1)}$	j	$u_a^{(1)}$
1	.0000	1	.263+01	2	.271+01	3	.295+01	4	.335+01	5	.407+01
2	.5000-01	1	.281+01	2	.289+01	3	.313+01	4	.356+01	5	.472+01
3	.1000+00	1	.312+01	2	.319+01	3	.341+01	4	.380+01	5	.481+01
4	.1500+00	1	.346+01	2	.353+01	3	.372+01	4	.405+01	5	.456+01
5	.2000+00	1	.376+01	2	.381+01	3	.397+01	4	.423+01	5	.463+01
6	.2500+00	1	.393+01	2	.397+01	3	.409+01	4	.429+01	5	.457+01
7	.3000+00	1	.391+01	2	.394+01	3	.403+01	4	.418+01	5	.437+01
8	.3500+00	1	.367+01	2	.370+01	3	.377+01	4	.388+01	5	.402+01
9	.4000+00	1	.324+01	2	.326+01	3	.332+01	4	.342+01	5	.353+01
10	.4500+00	1	.268+01	2	.269+01	3	.275+01	4	.283+01	5	.292+01
11	.5000+00	1	.207+01	2	.209+01	3	.212+01	4	.218+01	5	.226+01
1	.0000	6	.507+01	7	.654+01	8	.867+01	9	.118+02	10	.163+02
2	.5000-01	6	.520+01	7	.662+01	8	.866+01	9	.116+02	10	.160+02
3	.1000+00	6	.528+01	7	.654+01	8	.834+01	9	.109+02	10	.148+02
4	.1500+00	6	.528+01	7	.629+01	8	.772+01	9	.977+01	10	.128+02
5	.2000+00	6	.517+01	7	.590+01	8	.687+01	9	.819+01	10	.100+02
6	.2500+00	6	.494+01	7	.538+01	8	.588+01	9	.643+01	10	.695+01
7	.3000+00	6	.459+01	7	.479+01	8	.489+01	9	.474+01	10	.403+01
8	.3500+00	6	.414+01	7	.419+01	8	.403+01	9	.340+01	10	.192+01
9	.4000+00	6	.361+01	7	.361+01	8	.336+01	9	.259+01	10	.732+00
10	.4500+00	6	.301+01	7	.303+01	8	.289+01	9	.235+01	10	.942+00
11	.5000+00	6	.235+01	7	.242+01	8	.247+01	9	.244+01	10	.227+01

i	x position	j	$u_a^{(2)}$	j	$u_a^{(2)}$	j	$u_a^{(2)}$	j	$u_a^{(2)}$	j	$u_a^{(2)}$
1	.0000	1	-.681+00	2	-.693+00	3	-.729+00	4	-.789+00	5	-.871+00
2	.5000-01	1	-.135+01	2	-.136+01	3	-.142+01	4	-.152+01	5	-.167+01
3	.1000+00	1	-.185+01	2	-.187+01	3	-.195+01	4	-.205+01	5	-.231+01
4	.1500+00	1	-.213+01	2	-.216+01	3	-.226+01	4	-.243+01	5	-.272+01
5	.2000+00	1	-.218+01	2	-.222+01	3	-.234+01	4	-.255+01	5	-.29[illegible]+01
6	.2500+00	1	-.203+01	2	-.208+01	3	-.221+01	4	-.246+01	5	-.286+01
7	.3000+00	1	-.176+01	2	-.180+01	3	-.195+01	4	-.223+01	5	-.266+01
8	.3500+00	1	-.144+01	2	-.149+01	3	-.164+01	4	-.192+01	5	-.235+01
9	.4000+00	1	-.118+01	2	-.123+01	3	-.137+01	4	-.163+01	5	-.203+01
10	.4500+00	1	-.107+01	2	-.112+01	3	-.124+01	4	-.147+01	5	-.180+01
11	.5000+00	1	-.117+01	2	-.121+01	3	-.132+01	4	-.149+01	5	-.175+01
1	.0000	6	-.978+00	7	-.112+01	8	-.129+01	9	-.152+01	10	-.183+01
2	.5000-01	6	-.190+01	7	-.223+01	8	-.273+01	9	-.345+01	10	-.449+01
3	.1000+00	6	-.265+01	7	-.317+01	8	-.399+01	9	-.525+01	10	-.723+01
4	.1500+00	6	-.317+01	7	-.386+01	8	-.499+01	9	-.676+01	10	-.964+01
5	.2000+00	6	-.345+01	7	-.430+01	8	-.564+01	9	-.778+01	10	-.113+02
6	.2500+00	6	-.348+01	7	-.442+01	8	-.588+01	9	-.818+01	10	-.119+02
7	.3000+00	6	-.330+01	7	-.427+01	8	-.572+01	9	-.792+01	10	-.114+02
8	.3500+00	6	-.298+01	7	-.390+01	8	-.522+01	9	-.710+01	10	-.963+01
9	.4000+00	6	-.261+01	7	-.341+01	8	-.450+01	9	-.593+01	10	-.770+01
10	.4500+00	6	-.227+01	7	-.290+01	8	-.371+01	9	-.468+01	10	-.559+01
11	.5000+00	6	-.208+01	7	-.250+01	8	-.300+01	9	-.357+01	10	-.415+01

i	x position	j	$v_a^{(1)}$	j	$v_a^{(1)}$	j	$v_a^{(1)}$	j	$v_a^{(1)}$	j	$v_a^{(1)}$
1	.0000	1	-.303-03	2	.563-01	3	.113+00	4	.169+00	5	.276+00
2	.5000-01	1	-.893-03	2	.151+00	3	.314+00	4	.498+00	5	.721+00
3	.1000+00	1	-.145-02	2	.242+00	3	.506+00	4	.808+00	5	.118+01
4	.1500+00	1	-.190-02	2	.320+00	3	.670+00	4	.107+01	5	.156+01
5	.2000+00	1	-.216-02	2	.381+00	3	.795+00	4	.126+01	5	.183+01
6	.2500+00	1	-.217-02	2	.424+00	3	.880+00	4	.139+01	5	.200+01
7	.3000+00	1	-.187-02	2	.452+00	3	.933+00	4	.146+01	5	.208+01
8	.3500+00	1	-.129-02	2	.471+00	3	.965+00	4	.150+01	5	.210+01
9	.4000+00	1	-.572-03	2	.486+00	3	.988+00	4	.152+01	5	.210+01
10	.4500+00	1	.479-04	2	.497+00	3	.101+01	4	.154+01	5	.210+01
11	.5000+00	1	.304-03	2	.503+00	3	.101+01	4	.155+01	5	.211+01
1	.0000	6	.290+00	7	.369+00	8	.476+00	9	.626+00	10	.842+00
2	.5000-01	6	.101+01	7	.141+01	8	.198+01	9	.281+01	10	.406+01
3	.1000+00	6	.167+01	7	.235+01	8	.334+01	9	.481+01	10	.707+01
4	.1500+00	6	.221+01	7	.311+01	8	.442+01	9	.640+01	10	.953+01
5	.2000+00	6	.258+01	7	.361+01	8	.512+01	9	.741+01	10	.111+02
6	.2500+00	6	.279+01	7	.385+01	8	.540+01	9	.775+01	10	.115+02
7	.3000+00	6	.285+01	7	.386+01	8	.529+01	9	.742+01	10	.108+02
8	.3500+00	6	.281+01	7	.371+01	8	.490+01	9	.658+01	10	.910+01
9	.4000+00	6	.275+01	7	.350+01	8	.441+01	9	.551+01	10	.691+01
10	.4500+00	6	.270+01	7	.335+01	8	.401+01	9	.460+01	10	.492+01
11	.5000+00	6	.270+01	7	.330+01	8	.386+01	9	.422+01	10	.402+01

i	x position	j	$v^{(2)}$	j	$v^{(2)}$	j	$v^{(2)}$	j	$v^{(2)}$	j	$v^{(2)}$
1	.0000	1	-.258-02	2	.445+00	3	.950+00	4	.156+01	5	.235+01
2	.5000-01	1	-.177-02	2	.362+00	3	.772+00	4	.127+01	5	.191+01
3	.1000+00	1	-.647-03	2	.255+00	3	.541+00	4	.984+00	5	.132+01
4	.1500+00	1	.558-03	2	.134+00	3	.279+00	4	.453+00	5	.663+00
5	.2000+00	1	.158-02	2	.621-02	3	.115-01	4	.155-01	5	.379-02
6	.2500+00	1	.218-02	2	-.113+00	3	-.243+00	4	-.393+00	5	-.596+00
7	.3000+00	1	.222-02	2	-.223+00	3	-.470+00	4	-.748+00	5	-.110+01
8	.3500+00	1	.172-02	2	-.320+00	3	-.662+00	4	-.104+01	5	-.149+01
9	.4000+00	1	.899-03	2	-.401+00	3	-.820+00	4	-.127+01	5	-.176+01
10	.4500+00	1	.988-04	2	-.466+00	3	-.945+00	4	-.145+01	5	-.199+01
11	.5000+00	1	-.350-03	2	-.514+00	3	-.104+01	4	-.158+01	5	-.215+01
1	.0000	6	.342+01	7	.492+01	8	.708+01	9	.102+02	10	.150+02
2	.5000-01	6	.277+01	7	.396+01	8	.564+01	9	.806+01	10	.116+02
3	.1000+00	6	.189+01	7	.265+01	6	.367+01	9	.504+01	10	.694+01
4	.1500+00	6	.912+00	7	.119+01	8	.146+01	9	.166+01	10	.163+01
5	.2000+00	6	-.558-01	7	-.229+00	8	-.642+00	9	-.151+01	10	-.328+01
6	.2500+00	6	-.907+00	7	-.143+01	8	-.233+01	9	-.394+01	10	-.688+01
7	.3000+00	6	-.158+01	7	-.229+01	8	-.344+01	9	-.532+01	10	-.858+01
8	.3500+00	6	-.205+01	7	-.282+01	8	-.394+01	9	-.563+01	10	-.837+01
9	.4000+00	6	-.237+01	7	-.309+01	8	-.401+01	9	-.520+01	10	-.683+01
10	.4500+00	6	-.258+01	7	-.323+01	8	-.391+01	9	-.456+01	10	-.499+01
11	.5000+00	6	-.275+01	7	-.335+01	8	-.390+01	9	-.426+01	10	-.404+01

REFERENCES

1. Alfredson, R. J.: A Note on the Use of the Finite Difference Method for Predicting Steady State Sound Fields. Acoustica, vol. 28, no. 5, May 1973, pp. 296-301.

2. Baumeister, Kenneth J.; and Bittner, Edward C.: Numerical Simulation of Noise Propagation in Jet Engine Ducts. NASA TN D-7339, 1973.

3. Baumeister, Kenneth J.; and Rice, Edward J.: A Difference Theory for Noise Propagation in an Acoustically Lined Duct with Mean Flow. Aeroacoustics: Jet and Combustion Noise; Duct Acoustics, Henry T. Nagamatsu, J. V. O'Keefe and I. R. Schwartz, eds. (AIAA Progress in Astronautics and Aeronautics series, vol. 37.) The MIT Press, 1975, pp. 435-453.

4. Baumeister, Kenneth J.: Analysis of Sound Propagation in Ducts Using the Wave Envelope Concept. NASA TN D-7719, 1974.

5. Quinn, D. W.: A Finite Difference Method for Computing Sound Propagation in Nonuniform Ducts. AIAA paper 75-130, Jan. 1975.

6. Baumeister, Kenneth J.: Wave Envelope Analysis of Sound Propagation in Ducts with Variable Axial Impedance. Aeroacoustics: Duct Acoustics, Fan Noise and Control Rotor Noise, Ira R. Schwartz, Henry T. Nagamatsu, and Warren Strohle, eds. (AIAA Progress in Astronautics and Aeronautics Series, vol. 44.) The MIT Press, 1976, pp. 451-474.

7. Quinn, D. W.: Attenuation of Sound Associated with a Plane Wave in a Multisectioned Cylindrical Duct. Aeroacoustics: Duct Acoustics, Fan Noise and Control Rotor Noise, Ira R. Schwartz, Henry T. Nagamatsu, and Warren Strohle, eds. (AIAA Progress in Astronautics and Aeronautics Series, vol. 44.) The MIT Press, 1976, pp. 331-345.

8. Sigman, R. K.; Majjigi, R. K.; and Zinn, B. T.: Use of Finite Element Techniques in the Determination of the Acoustic Properties of Turbofan Inlets. AIAA paper 77-18, Jan. 1977.

9. Motsinger, R. E.; et al.: Optimization of Suppression for Two-Element Treatment Liners for Turbomachinery Exhaust Ducts. (R76AEG256, General Electric Co.; NAS3-18555.) NASA CR-134997, 1976.

10. Kaiser, J. E.; and Nayfeh, A. H.: A Wave-Envelope Technique for Wave Propagation in Non-uniform Ducts. AIAA Paper 76-496, July 1976.

11. Mungur, P.; and Gladwell, G. M. L.: Acoustic Wave Propagation in a Sheared Fluid Contained in a Duct. J. Sound Vib., vol. 9, no. 1, Jan. 1969, pp. 28-48.

12. Morfey, C. L.: Acoustic Energy in Non-uniform Flows. J. Sound Vib., vol. 14, no. 2, Feb. 1971, pp. 159-170.

13. Goldstein, Marvin E.: Aeroacoustics. McGraw-Hill International Book Co., 1976.

14. Ryshov, O. S.; and Shefter, G. M.: On the Energy of Acoustic Waves Propagating in Moving Media. J. Appl. Math. Mech. (Engl. Transl.), vol. 26, no. 5, 1962, pp. 1293-1309.

15. Morse, Philip McCord: Vibration and Sound. Second Ed., McGraw-Hill Book Co., Inc., 1948.

16. Dwight, Herbert Bristol: Table of Integrals and Other Mathematical Data. Revised ed. The Macmillan Company, 1947.

TABLE I. - COEFFICIENTS IN DIFFERENCE EQUATION (EQ. (54))

Cell index, k	Matrix element				
	a_k	b_k	c_k	d_k	e_k
1	$-K_1\left(\frac{\Delta y}{\Delta x}\right)^2 + K_3\frac{(\Delta y)^2}{2\,\Delta x}$	-1	$2\left[1 + K_1\left(\frac{\Delta y}{\Delta x}\right)^2 - \frac{K_2(\Delta y)^2}{2}\right]$	-1	$-K_1\left(\frac{\Delta y}{\Delta x}\right)^2 - K_3\frac{(\Delta y)^2}{2\,\Delta x}$
2	$a_1 + W_2\frac{\Delta y}{\Delta x} - 2W_3\frac{\Delta y}{(\Delta x)^2}$	-2	$c_1 - 2W_1\,\Delta y + 4W_3\frac{\Delta y}{(\Delta x)^2}$	0	$e_1 - W_2\frac{\Delta y}{\Delta x} - 2W_3\frac{\Delta y}{(\Delta x)^2}$
3	a_2	0	c_2	-2	e_2
4	$2a_1$	$-1 - \frac{2K_1L_2}{\Delta x}$	$c_1 - \frac{K_3\,\Delta y^2}{\Delta x} + \frac{4K_1L_2}{\Delta x} - \frac{2K_1L_1(\Delta y)^2}{\Delta x}$	$-1 - \frac{2K_1L_2}{\Delta x}$	0
5	$a_4 + 4K_1L_2N_2\frac{\Delta y}{(\Delta x)^2} + 2N_2\frac{\Delta y}{\Delta x}$	$2b_4$	$c_4 - 2N_1\,\Delta y - 2N_2\frac{\Delta y}{\Delta x} - 4K_1L_2N_1\frac{\Delta y}{\Delta x} - 4K_1L_2N_2\frac{\Delta y}{(\Delta x)^2}$	0	0
6	a_5	0	c_5	b_5	0

TABLE II. - SUMMARY OF OPTIMIZATION

RESULTS (REF. 9)

[Length-height ratio, L^*/H^*, 3.43; Mach number, M, 0.3; plane-wave source.]

Dimensionless frequency, η	Specific acoustic impedance, ζ	Sound attenuation, Δ dB, dB
0.5	0.31 - 0.1 i	70.6
1.0	.65 - .5 i	39.2
1.535	.85 - 1.0 i	22.6
2.0	.90 - 1.4 i	14.3
5.0	.85 - 2.45 i	4.0
10.0	1.40 - 3.6 i	2.30

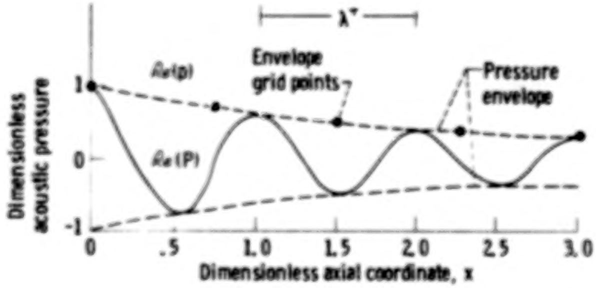

Figure 1. - Typical pressure profile for sound propagation in two-dimensional, soft-wall duct. Dimensionless frequency, η, 1; dimensionless duct length, L^*/H^*, 3.

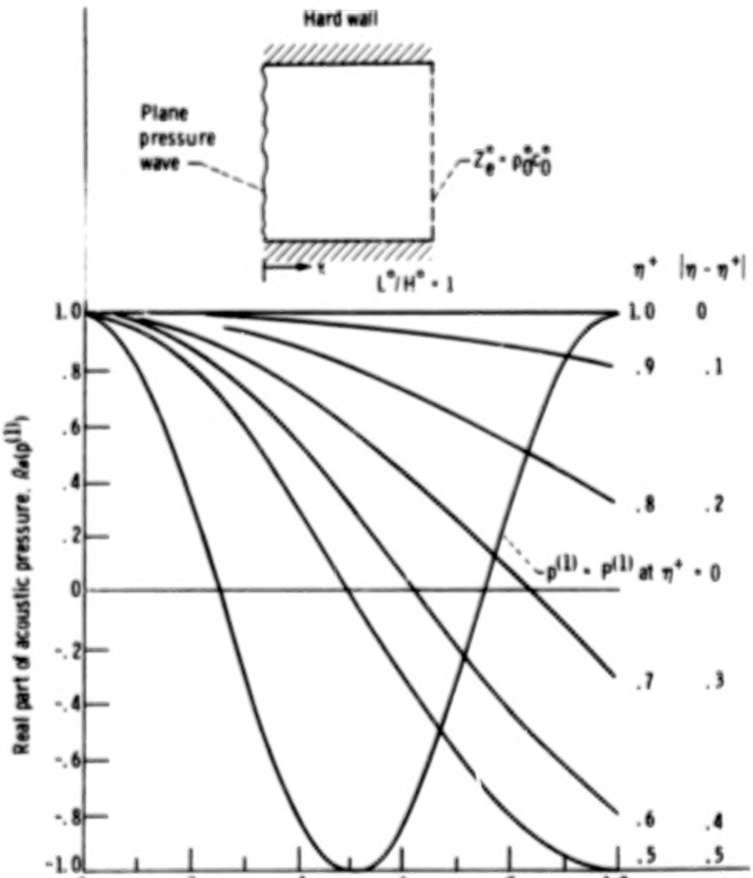

Figure 2. - Sensitivity of real pressure component $p^{(1)}$ to choice of wave envelope of frequency η^+ for two-dimensional hard-wall duct. Dimensionless frequency, η, 1; dimensionless duct length, L^*/H^* = 3.

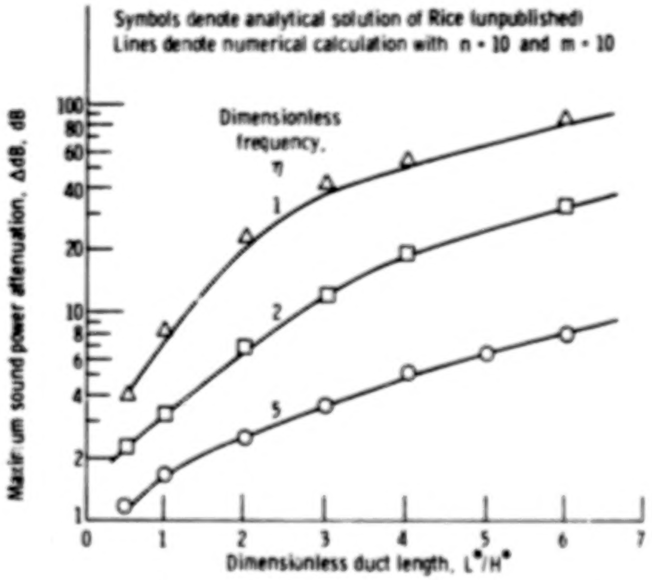

Figure 3. - Effect of axial duct length and dimensionless frequency on attenuation at optimum impedance in two-dimensional, soft-wall duct assuming that wave envelope frequency η^+ equals η. (From ref. 4.)

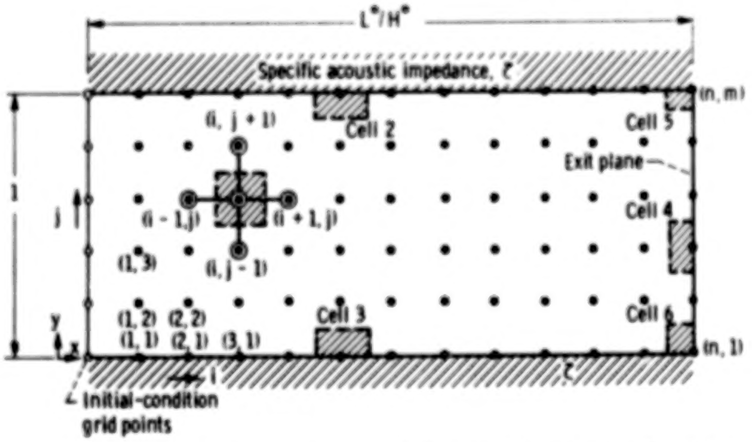

Figure 4. - Coordinate and grid-point representation of two-dimensional, soft-wall duct.

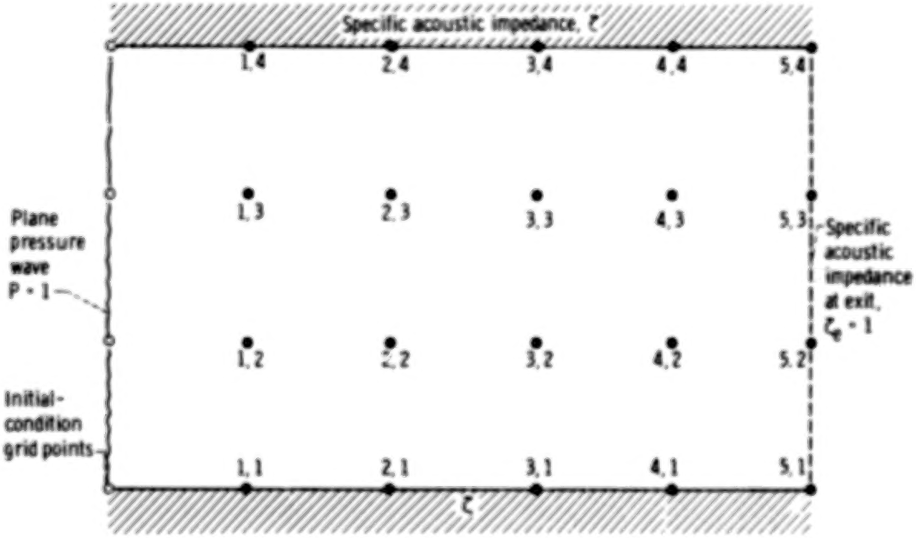

Figure 5. - Illustrative example of soft-wall duct with total number of grid rows m of 4 and total number of grid columns n of 5.

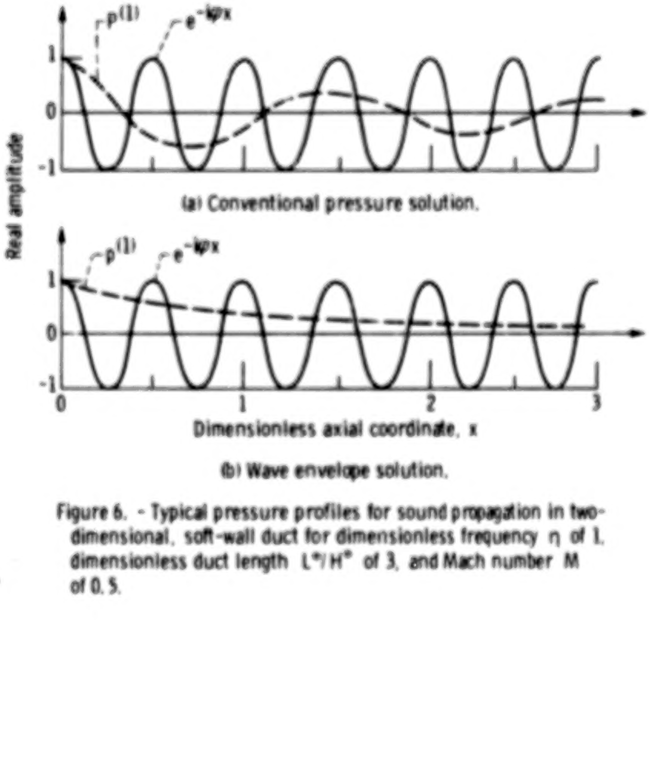

Figure 6. - Typical pressure profiles for sound propagation in two-dimensional, soft-wall duct for dimensionless frequency η of 1, dimensionless duct length L^*/H^* of 3, and Mach number M of 0.5.

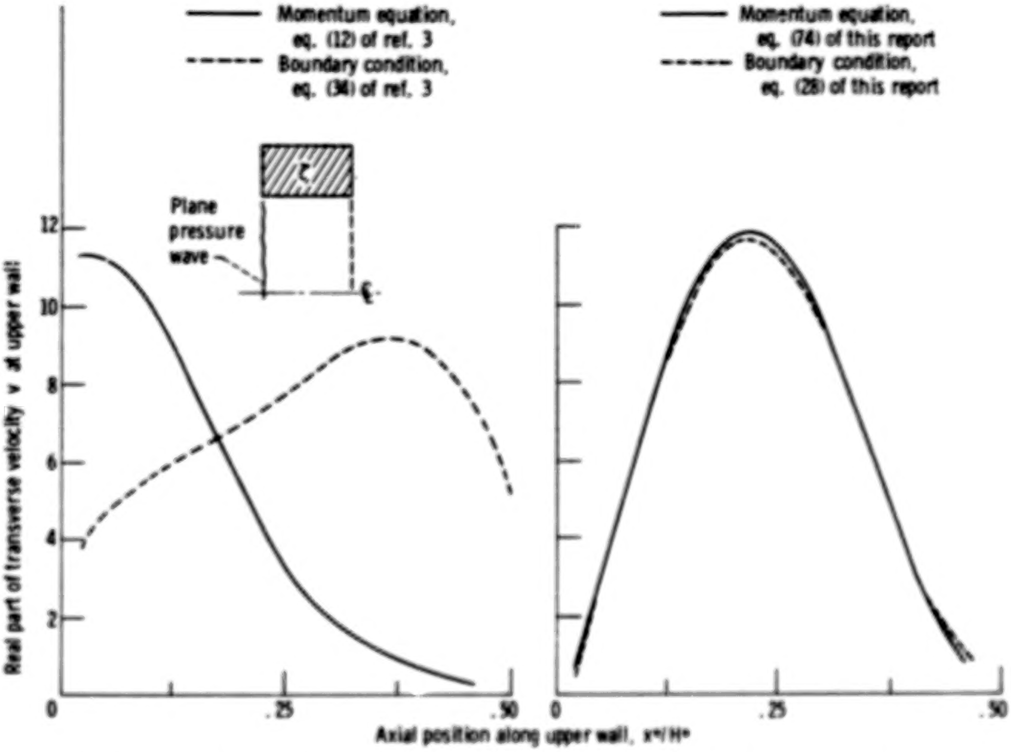

(a) Exit condition of reference 3. Sound attenuation, ΔdB, 6.1 decibels.

(b) Exit condition of this report. Sound attenuation, ΔdB, 3.4 decibels.

Figure 7. - Comparison of dimensionless transverse acoustic particle velocity v at wall as calculated from momentum equation and impedance condition. Dimensionless frequency, η, 0.6; dimensionless duct length, L^*/H^*, 0.5; Mach number, M, 0.5; specific acoustic impedance, ζ, 0.071 - i 0.151.

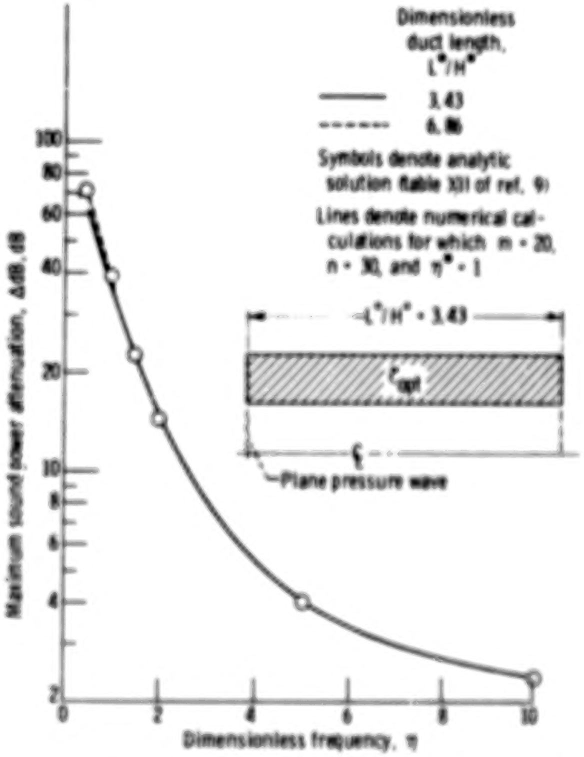

Figure 8. - Effect of dimensionless frequency on attenuation at optimum impedance in two-dimensional soft-wall duct. Dimensionless duct length, L^*/H^*, 3.43; Mach number, M, 0.3.

1. Report No.	2. Government Accession No.	3. Recipient's Catalog No.
NASA TP-1001		

4. Title and Subtitle	5. Report Date
FINITE-DIFFERENCE THEORY FOR SOUND PROPAGATION IN A LINED DUCT WITH UNIFORM FLOW USING THE WAVE ENVELOPE CONCEPT	August 1977
	6. Performing Organization Code
7. Author(s)	8. Performing Organization Report No.
Kenneth J. Baumeister	E-9149
	10. Work Unit No.
9. Performing Organization Name and Address	505-03
National Aeronautics and Space Administration Lewis Research Center Cleveland, Ohio 44135	11. Contract or Grant No.
	13. Type of Report and Period Covered
12. Sponsoring Agency Name and Address	Technical Paper
National Aeronautics and Space Administration Washington, D.C. 20546	14. Sponsoring Agency Code

15. Supplementary Notes

16. Abstract

The finite-difference equations are derived for sound propagation in a two-dimensional, straight, soft-wall duct with a uniform flow by using the wave envelope concept. This concept reduces the required number of finite-difference grid points by one to two orders of magnitude depending on the length of the duct and the frequency of the sound. In this report, the governing acoustic-difference equations in complex notation are derived. Also, a new exit condition is developed that allows a duct of finite length to simulate the wave propagation in an infinitely long duct. Sample calculations are presented for a plane wave incident upon the acoustic liner. They show the numerical theory to be in good agreement with closed-form analytical theory. Also, complete pressure and velocity printouts are given to some sample problems and can be used to debug and check future computer programs.

17. Key Words (Suggested by Author(s))	18. Distribution Statement
Finite difference; Sound propagation; Attenuation; Uniform flow	Unclassified - unlimited STAR Category 71

19. Security Classif. (of this report)	20. Security Classif. (of this page)	21. No. of Pages	22. Price*
Unclassified	Unclassified	64	A04

* For sale by the National Technical Information Service, Springfield, Virginia 22161